SSRMP Annual Scientific Meeting 2018

22th and 23th November 2018

CHUV – Lausanne

Schweizerische Gesellschaft für Strahlenbiologie und Medizinische Physik
Société Suisse de Radiobiologie et de Physique Médicale
Società Svizzera di Radiobiologia e di Fisica Medica
Swiss Society of Radiobiology and Medical Physics

SGSMP
SSRPM
SSRFM


PLAN
VISUALIZATION
PLAN
EVALUATION
PLAN
VERIFICATION
AND
3D Monte Carlo
THERE IS A NEW INTELLIGENCE IN TOWN.
VERIQA
MISSION:PATIENT QA
STARRING
VISUALIZATION
EVALUATION
VERIFICATION
AND
3D MONTE CARLO
PTW DOSIMETRY INTELLIGENCE PRESENTS A ONE-STOP SOLUTION PRODUCTION "VERIQA SMART PATIENT QA" FEATURING ONE SINGLE MODULAR PLATFORM
FULLY AUTOMATED WORKFLOWS · FAST WEB-BASED ACCESS TO RESULTS · INDEPENDENT MONTE CARLO DOSE CALCULATIONS
4D PHANTOM MEASUREMENTS AND TRACK-IT DATA MANAGEMENT · ALL IN ONE MULTI-TASKING PLATFORM
COMING SOON
WWW.VERIQA.DE
PTW

Bienvenue à Lausanne

Nous nous réjouissons de vous accueillir à Lausanne dans le cadre de notre congrès annuel les 22 et 23 novembre 2018.

Nous avons préparé un programme attrayant dans tous les domaines de la physique médicale. L'automatisation et l'intelligence artificielle seront les sujets principaux du congrès et seront abordés par deux conférenciers invités de renom. Ce programme est complété par un grand nombre d'exposés des membres de notre société. Nous remercions à avance tous les conférenciers.

L'assemblée annuelle de la SSRPM aura lieu le jeudi 22 novembre 2018 à 16h30. Ce sera l'occasion de faire le point sur la position de la physique médicale en Suisse et de renouveler les membres de notre comité.
Je remercie chaleureusement nos sponsors pour le soutien financier. Sans eux, le congrès ne pourrait pas avoir lieu gratuitement pour nos membres.
Au nom du comité d'organisation, je vous souhaite un excellent congrès.

Pour le comité d'organisation

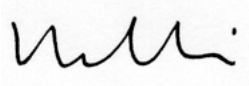

R. Moeckli

General Informations

Location

CHUV - Centre Hospitalier Universitaire Vaudois

Auditoire BH08 3 - Charlotte Olivier

Rue du Bugnon 44

CH 1011 Lausanne

Organising Committee

R. Moeckli (chair), P. Manser, F. Bochud, F. Verdun, C. Bailat, J. Damet, V. Vallet

Contacts

Nicole Tille (Administration)

Nicole.Tille@chuv.ch, tel. : +41 21 314 82 41

Raphaël Moeckli (General organisation)

Raphael.Moeckli@chuv.ch, tel. : +41 21 314 46 18

Access

By train : Arrival to Lausanne railway station – Métro M2 in front of the station, direction « Croisettes », exit station « CHUV ».

By car : Highway exit « Lausanne-Vennes » ; follow direction « hôpitaux » ; parking very difficult near CHUV ; public parking expensive.

Hotel

Please contact Lausanne Tourisme

www.lausanne-tourisme.ch, tel : +41 21 613 73 73.

Diner

The evening diner will take place at « Chalet Suisse » http://www.chaletsuisse.ch

CHUV

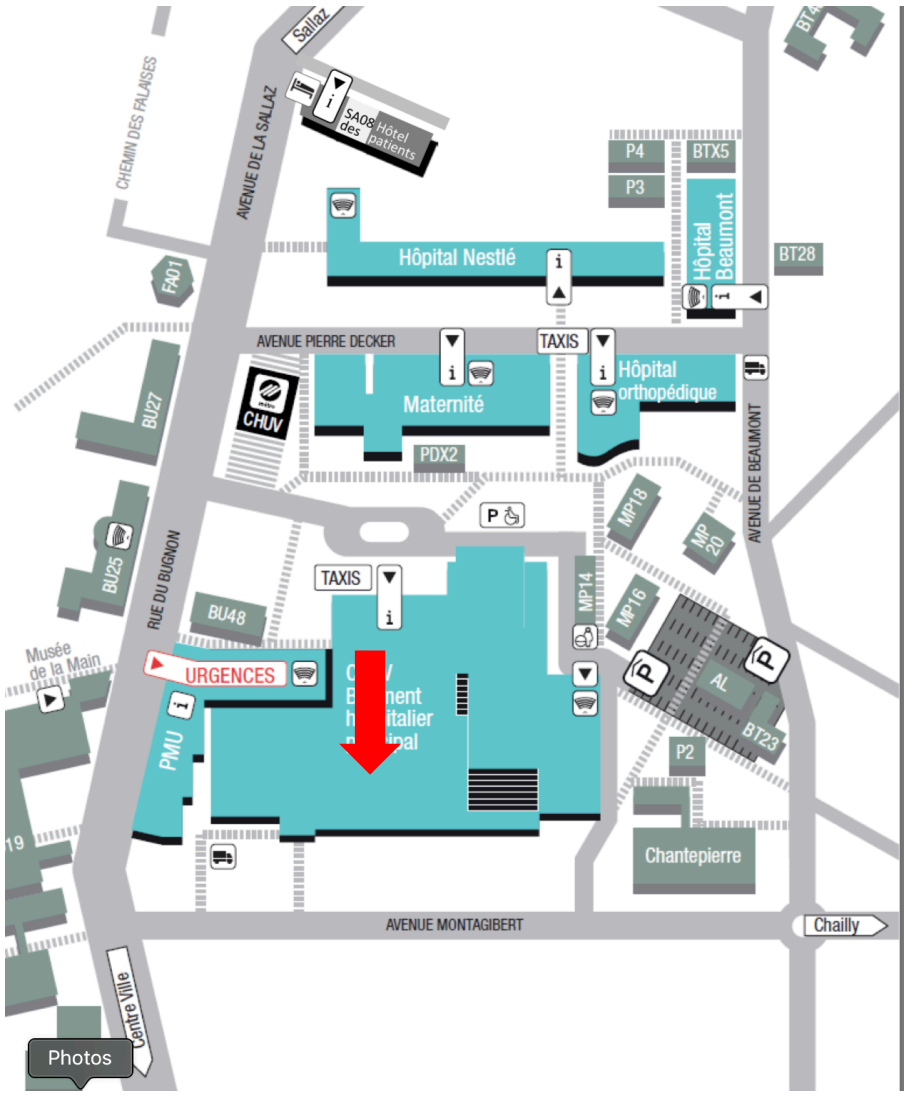

Chalet Suisse

Only a few minutes from the center of Lausanne.

Motorway to Lausanne-Nord, exit Vennes

Metro + Bus
Section Grand-Vennes, "Signal" stop

~18:34 m2 18:39	CHUV Lausanne Lausanne-Gare **Riponne-M.Béjart**
~18:41 7 18:43	Riponne-M.Béjart Pully, Val-Vert **Tunnel**
~18:50 16 18:56	Tunnel Grand-Vennes **Signal**

Exhibitors and sponsors

Accuray

Brainlab

Conmedica/Scandidos

Elekta

Meditron

PTW

Qualiformed

Raditec

RaySearchLabs

Solumedics

Varian

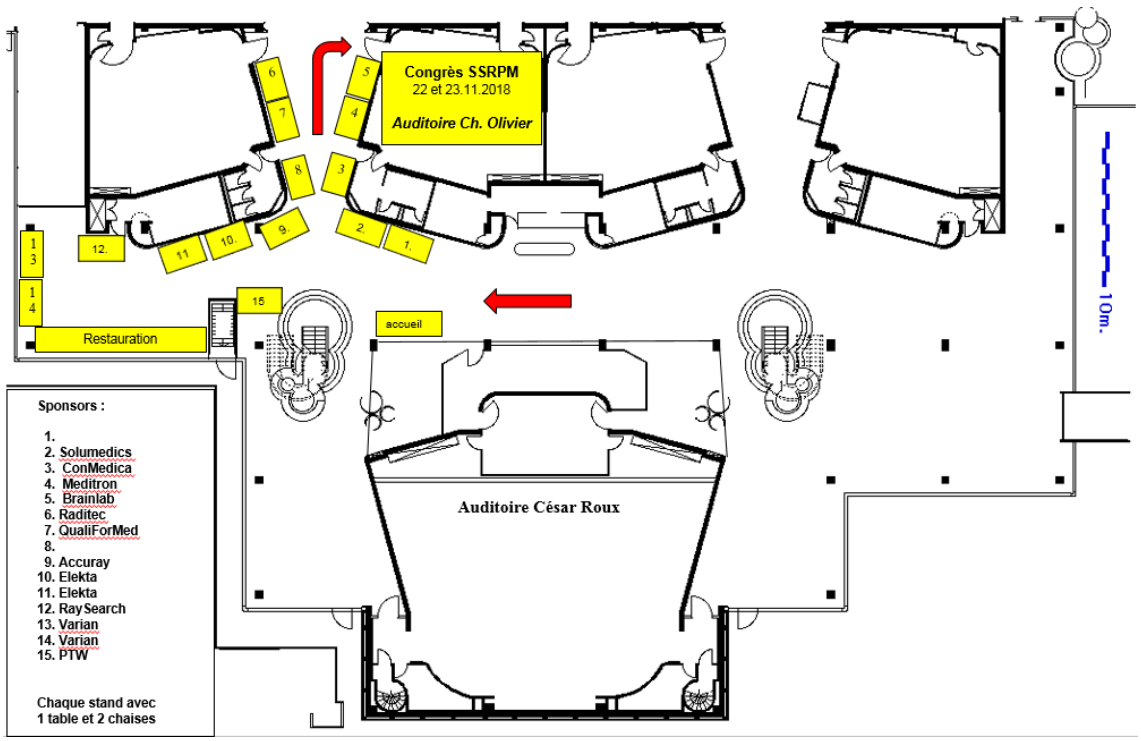

Program

Thursday 22nd Novembre

0900 - 1000 **Registration**

1000 - 1015 **Opening of the meeting**
R. Moeckli, Organising committee, Lausanne
P. Manser, SSRMP president, Bern

1015 - 1215 **Radiotherapy I**
Chair : M. Jaccard, Genève

1015 U. Schneider, Hirslanden Zürich
Tumor Size can have an Impact on the Outcomes of Epidemiological Studies on Second Cancers after Radiotherapy

1030 N. Corradini, Clinica luganese, Lugano
Accuracy of dynamic jaw field widths on TomoTherapy

1045 C. Winterhalter, Paul Scherrer Institute, Villigen
Replacing patient specific quality assurance measurements with log file based Monte Carlo simulations for proton therapy

1100 R. Kueng, Inselspital, Bern
Dosimetric implications of Geant4 version changes for proton radiation therapy

1115 N. Bizzocchi, Paul Scherrer Institute, Villigen
Spot and layer spacing optimization for proton pencil beam scanning with Eclipse TPS

1130 Z. Girbau, Kantonsspital Aarau, Aarau
Is Monte Carlo planning really justified in intracranial radiosurgery?

1145 P. Gonçalves Jorge, Institut de Radiophysique, Lausanne
Beam monitoring through out-of-field measurements in a pulsed electron beam at ultra-high dose-rate

1200 N. Koutsoulevis, Hôpital Universitaire, Geneva
Quality assurance of small animal irradiation: validation of a 3D-printed phantom for delivered dose evaluation

1215 - 1330 **Lunch posters and Industrial exhibition**

Thursday 22nd Novembre

1330 - 1445	**Nuclear medicine, radiation protection, radiation metrology, radiobiology** *Chair : S. Presilla, Bellinzona*
1330	S. Gnesin, Institut de Radiophysique, Lausanne *Phantom-based image quality assessment and clinical protocol optimization in SiPM PET/CT and comparison with conventional PMT-based PET/CT devices*
1345	K. Shi, Inselspital, Bern *Deep Learning for the Detection of Lesions on ^{68}Ga-PSMA PET/CT Imaging*
1400	M. Gondré, Institut de Radiophysique, Lausanne *Optimization of alanine dosimetry for doses from 10Gy to 100Gy for flash-beam radiotherapy*
1415	P. Montay-Gruel, CHUV, Lausanne *FLASH Radiotherapy: Spare the normal tissue but not the tumor by oxygen-dependent mechanisms*
1430	L. Bellesi, Ospedale Regionale, Bellinzona *How and why is the medical physicist unit of radioprotection useful in a radiology department ? A quantitative analysis*
1445 - 1515	**Coffee,posters,exhibition (Sponsored by Elekta)**
1515 - 1630	**Radiological physics I** *Chair : E. Samara, Sion*
1515	A. Viry, Institut de Radiophysique, Lausanne *Diagnosis of crystal-related arthropathies with a multi-energy spectral photon counting CT*
1530	T. Lima, Kantonsspital, Aarau *Clinical impact of CT protocol optimisation in adaptive radiotherapy*
1545	D. Racine, Institut de Radiophysique, Lausanne *Optimization of abdominal CT protocols using a model observer: a multi-centric quantitative analysis*
1600	C. Aberle, Universitätsspital, Basel *Update of the Diagnostic Reference Levels for CT in Switzerland with Dose Management Software*
1615	T. Lima, Kantonsspital, Aarau *Swiss National CT Dose Registry*
1630 1800	**Annual general assembly SSRMP**
1900	**Dinner at Chalet Suisse (with the kind support of Elekta, Varian, Solumedics and RaySearch)**

Friday 23nd Novembre 2018

0830 - 1015 **Radiological Physics II**
Chair : D. Racine, Lausanne

0830 T. Roggen, Varian Medical Systems, Daettwil
Machine Learning based Feature Detection on 2D X-Ray Images

0845 E. Samara, Hôpital du Valais, Sion
Why is it important to connect all X-ray units to a dose management system?

0900 M. Sans Merce, Hôpital Universitaire, Genève
Dosimetric evaluation of the O-arm imaging system

0915 N. Ryckx, Institut de Radiophysique, Lausanne
Assessment of the efficiency in eye and brain dose reduction of a leaded facemask in clinical conditions using an anthropomorphic phantom and TLD

0930 Invited speaker : M. Reyes, Bern
Deep learning in medical physics : Where are we ? Challanges and opportunities

1015 - 1100 **Coffee, exhibition (Sponsored by RaySearch)**

1100 - 1300 **Radiotherapy II**
Chair : M. Fix, Bern

1100 Invited speaker : B. Heijmen, Erasmus MC, Rotterdam
Automation in radiation therapy planning : the existing and the future

1145 M. Bogowitz , Universitätsspital, Zürich
CT lymph node radiomics improves prediction of locoregional control in head and neck cancer

1200 D. Vuong, Universitätsspital, Zürich
Do we need standardized imaging protocols or robust radiomic features for the development of image-biomarker based prognostic models?

1215 L. Halter , Inselspital, Bern
Modeling the radiation transport in a prototype MRI-Linac system using the Monte Carlo technique

1230 E. Colwill, Paul Scherrer Institute, Villigen
Anthropomorphic phantom with lung and liver compartments for MR guided radiation therapy

1245 S. Mueller, Inselspital, Bern
Deliverability-verification of treatment plans for dynamic mixed beam radiotherapy (DYMBER)

Friday 23nd Novembre 2018

1300 - 1415 **Lunch, coffee, posters, exhibitions (Sponsored by Varian)**

1415 - 1600 **Radiotherapy III**
Chair : F. Belosi, Villigen

1415 S. Thengumpallil, Clinique des Grangettes, Genève
Towards personalized radiotherapy imaging dose report: a phantom-based evaluation of dose exposure

1430 M. Jaccard, Hôpital Universitaire, Genève
Electromagnetic transponders for real-time tracking in lung stereotactic radiotherapy: first clinical experience

1445 F. Emert, Paul Scherrer Institute, Villigen
How risky is 4D planning? – A FMEA based human error comparison of planning risks in 3D/4D proton therapy QA performed at CPT/PSI

1500 P. Logaritsch, Kantonsspital, Luzern
A quantitative evaluation of (deformable) image registration accuracy following AAPM TG 132

1515 S. Ehrbar, Universitätsspital, Zürich
ELPHA: Dynamically deformable liver phantom

1530 R. Kueng, Inselspital, Bern
Implementation of an efficient in-house tool for patient-specific quality assurance in HDR brachytherapy

1545 F. Amstutz, Universitätsspital, Zürich
Impact of tumor motion on robustness of radiomic features - comparison of PET and CT

1600 - 1615 **Closing of the meeting**
P. Manser, SSRMP president, Bern

Unleash your ability to deliver high-precision SRS treatments

HyperArc™ high-definition radiotherapy technology is designed to simplify even the most complex non-coplanar SRS treatments. Experience leading-edge features that allow you to treat multiple metastases simultaneously, enhancing your ability to treat more patients, reduce treatment times, increase throughput and maximize efficiency.

Learn more at: Varian.com/HyperArc

Safety information: Radiation may cause side effects and may not be appropriate for all cancers.

varian

Abstracts – Posters presentations

P01 **Contraindication for radiative deep regional hyperthermia for patients with large carbon implants**

Marder D. (1), Poel R. (2), Gisep A. (3), Van Stam G. (1), Timm O. (1), Puric E. (1), Datta N.R. (1), Lutters G. (1)
(1) Kantonsspital Aarau, Radio-Onkologie-Zentrum KSA-KSB, Aarau, Switzerland
(2) Paul Scherrer Institute, Villigen, Switzerland
(3) icotec AG, Altstätten, Switzerland

P02 **GLAaS absolute dose calibration algorithm with Elekta iViewGT Electronic Portal Imaging Device (EPID): multi-institute first experiences**

Eugenio Vanetti (1), Marco Esposito (2), Juan Maria Perez (3), Stefano Ren Kaiser (4), Giorgia Nicolini(1)
(1) Radiqa Developments, Medical Physics Team, Bellinzona, Switzerland
(2) SC Fisica Sanitaria, Usl Toscana centro, Firenze, Italy
(3) Servicio de Radiofísica, Hospital Universitario HM Puerta del Sur, Móstoles (Madrid), Spain
(4) Servizio di Fisica Sanitaria, Fondazione Poliambulanza Istituto Ospedaliero, Brescia, Italy

P03 **Treating breast cancer with VMAT in deep inspiration breath hold: the Geneva experience**

A. Dubouloz (1), P. Nouet (1), N. Koutsouvelis (1), G. Dipasquale (1), M. Jaccard (1), O. Fargier-Bochaton (1), M. Rouzaud (1)
(1) Radiation Oncology/Geneva University Hospitals, Geneva/Switzerland

P04 **Shortening delivery times for PBS proton therapy by reducing the number of proton spots without compromising dosimetric plan quality**

Maria F. Belosi, MSc [1]; Steven van de Water, PhD [1], Francesca Albertini, PhD [1]; Damien C. Weber, MD [1]; and Antony J. Lomax, PhD [1]
[1] Center for Proton Therapy, Paul Scherrer Institute, 5232 Villigen PSI, Switzerland

P05 **Evaluation of the pre and post-treatment positioning accuracy of patients treated in Gantry 2**

L.Mikroutsikos, L.Marc, F.Albertini, D.C. Weber, T.Lomax, A.Bolsi,
Paul Scherrer Institute

P06 **Statistical assessment of intrafractional interruptions during DIBH left-breast treatments**

Lia Vugts, Sofia Celi, Nicoletta Lomax, Kirsten Steinauer, Gerd Lutters
Radio-Onkologie Zentrum KSA-KSB

P07 **Supine or prone-crawl photon and proton RT plans for breast and regional lymph node including the IM chain**

Francesca Belosi[2, $], Bruno Speleers[1,$], Werner De Gersem[1], Pieter Deseyne[3], Leen Paelinck[3], Alessandra Bolsi[2], Anthony Lomax[2], Bert Boute[5], Annick Van Greveling[3], Christel Monten[1,3], Joris Van de Velde[4], Tom Vercautere [1,3] , Liv Veldeman [1,3], Damien Charles Weber[2,6] and Wilfried De Neve [1,3,$]
[$]contributed equally
[1]Department of Radiotherapy and Experimental Cancer Research, Faculty of Medicine and Health Sciences, Ghent University, Belgium
[2]Paul Scherrer Institut, Villigen, Switzerland
[3]Department of Radiation Oncology, University Hospital Ghent, Belgium
[4]Department of Anatomy, Faculty of Medicine and Health Sciences, Ghent University, Belgium
[5]Industrial Design Center, Faculty of Engineering and Architecture, Ghent University, Belgium
[6]Radiation Oncology, University Hospital of Bern, Inselspital, Bern

P08 **Portal Dosimetry with the 43 cm x 43 cm MV Imager: Improving Large-Field Performance by Diagonal Profile Adjustments**

Thomas Buchsbaum (1), Federico Hasenbalg (1)
(1) Stadtspital Triemli Zürich, Radio-Onkologie, CH-8063 Zürich, Birmensdorferstrasse 497

P09 **Dosimetric Impact of Titanium and Carbon Implants in Photon Therapy**

N. Klippel (1), D. Terribilini (1), A. Gisep (2), A. Joosten (1), H. Hemmatazad (1), K. Zaugg (3), D.M. Aebersold (1), P. Manser (1)
(1) Division of Medical Radiation Physics and Department of Radiation Oncology, Inselspital, Bern University Hospital, Switzerland
(2) icotec AG, Altstätten, Switzerland
(3) Klinik für Radio-Onkologie, Stadtspital Triemli, Zürich, Switzerland

P10 **Hybrid Intensity Modulated Treatment based on Gradient Fluence Maps: Application to loco regional breast cancer**
R. Boucenna, ***N. Pitteloud****, M. Betz*
Clinique Bois-Cerf Hirslanden Lausanne

P11 **EPR-Imaging of magnetic field induced dose effects at air cavities**
Sebastian Höfel (1,2), Michael K. Fix (3), Felix Zwicker (2), Malte Drescher (1)
(1) Department of Chemistry, University of Konstanz, Germany
(2) Klinik für Strahlentherapie/Radiologische Gemeinschaftspraxis, Gesundheitsverbund Landkreis Konstanz, Konstanz, Germany
(3) Division of Medical Radiation Physics and Department of Radiation Oncology, Inselspital, Bern University Hospital and University of Bern, Switzerland

P12 **Suitability of DDC for CT protocol optimisation with abdominal and head phantom**
Christian Sommer (1), Ismail Oezden (2), Thiago Lima (2), Mathias S. Weyland (1), Gerd Lutters (2), Stephan Scheidegger (1,2)
(1) ZHAW School of Engineering, Winterthur, Switzerland
(2) Kantonsspital Aarau, Switzerland

P13 **Multi-dimensional analysis of OSMS data during DIBH treatments**
H. Schneider, N. Lomax, G. Lutters
(1) Radio-Onkologie-Zentrum KSA-KSB

P14 **VMAT applied to synchronous bilateral breast cancer radiotherapy: dosimetric study on DIBH versus FB set up**
D. Gaudino[1], S. Cima[2], M. Frapolli[2], D. Daniele[2], B. Muoio[2], G.A. Pesce[2], F. Martucci[2], N.C. Azinwi[2], D. Bosetti[2], L. Bellesi[1], M. Casiraghi[1], M.A. Piliero[1], F. Pupillo[1], A. Richetti[2], M.C. Valli[2], S. Presilla[1].
(1) Ente Ospedaliero Cantonale, Medical Physics Unit, Bellinzona, Switzerland.
(2) Oncology Institute of Southern Switzerland, Radiation Oncology, Bellinzona-Lugano, Switzerland

P15 **Brain sparing through iterative single isocentre planning for multiple brain metastases**
Nicoletta Lomax, Sara Alonso, Mauricio Leick, Susanne Rogers, Gerd Lutters
Radio-Onkologie-Zentrum KSA-KSB, Kantonsspital Aarau

Abstracts – Oral presentations

Session Radiotherapy I

Tumor Size can have an Impact on the Outcomes of Epidemiological Studies on Second Cancers after Radiotherapy

Uwe Schneider (1,2), Linda Walsh (2), Wayne Newhauser (3)

(1) Radiotherapy Hirslanden, Witellikerstrasse 40, Zürich, Switzerland;
(2) Department of Physics, Science Faculty, University of Zürich, Switzerland;
(3) Department of Physics and Astronomy, Louisiana State University and Agricultural and Mechanical College, Baton Rouge, LA 70803 4001, USA;

Introduction

Many challenges are associated with obtaining a correct dose-response relationship for radiation induced cancer after radiotherapy with an epidemiological study. In order to gain a better understanding, some aspects of an epidemiological study on breast cancer following radiotherapy of Hodgkin's disease were simulated with Monte-Carlo methods.

Materials and Methods

Linear and non-linear mechanistic models which predict risk of cancer induction as a function of dose were applied randomly to a typical treatment plan. The study aspects chosen for consideration with simulations were the sizes and locations of the second tumor and the predicted radiation doses to the second tumor. The simulations provided information on how the dose variations can be directly influenced by the tumor size variations.

Results

The resulting study risk to predicted-dose-response-characteristic was analyzed. If a linear dose-response relationship for cancer induction was applied to calculate the theoretical doses at the simulated cancer sites, all Monte-Carlo realizations of the epidemiological study yielded strong evidence for a linear risk to predicted-dose-response. However, if a non-linear dose-response of cancer induction was applied to calculate the theoretical doses, the Monte Carlo simulated epidemiological study resulted in a non-linear risk to predicted-dose-response relationship only if the tumor size was small (< 1.5 cm). If the diagnosed breast cancers exceeded an average diameter of 1.5 cm, an applied non-linear mechanistic theoretical-dose-response relationship for second cancer falsely resulted in strong evidence for a linear predicted-dose relationship from the epidemiological study realizations. For a typical distribution of breast cancer sizes, the model selection probability for a predicted-dose linear model was 61% although a mechanistic non-linear theoretical-dose-response relationship for cancer induction had been applied.

Accuracy of dynamic jaw field widths on TomoTherapy

Nathan Corradini, Patrizia Urso, Cristina Vite

Centro di Radioterapia, Clinica Luganese Moncucco, Lugano, CH

Introduction
Dynamic jaw delivery, TomoEDGE™, on the TomoTherapy platform is an effective tool to decrease the patient dose along the superior and inferior edges of the treatment target. The TomoEDGE™ beam model uses 10 longitudinal beam profiles to model the dynamic jaw movement. This study aimed to provide an evaluation of the dynamic jaw accuracy over a 2 year period.

Materials and Methods
This study was performed on a TomoHDA machine and used the TQA Field Width Dynamic Jaws procedure for dose profile measurement. The procedure was run 84 times for a total of 840 dose profiles. Matlab software was used to analyze the measured dose profile data and to compare with those of the TomoEDGE™ beam model reference profiles. The full width half maximum (FWHM) was calculated for each profile and the comparison against reference was interpreted using the 1% tolerance limit recommended in the AAPM TG-148 report. In addition, the beam profile constancy was calculated for each field width.

Results
The mean reported FWHMs are observed to be within the TG-148 tolerance recommendation. A systematic difference of the FWHMs from reference values, 0.07 mm, can be seen throughout all the profiles. Individual FWHM measurements were outside the TG-148 tolerance for 22.6% (n = 19), 11.9% (n = 10), 28.6% (n = 24), 7.1% (n = 5) of all cases for the 2.0 +IEC, 1.0, 1.0 +IEC, and 1.0 −IEC FWs, respectively. Regarding constancy, symmetric FWs results were within 3% of reference in 95.2% (n = 320) of measurements, while only 63.9% (n = 322) of asymmetric FW measurements were within the 3% criteria, which increased to 94.8% (n = 398) with an expanded criteria of 4%.

Conclusion
This 2-yr study showed that the measured FW dose profiles of the TomoEDGE beam model respect the current AAPM TG-148 FWHM tolerance limit of 1% in most cases. However, the asymmetric FWs were unable to consistently satisfy the AAPM TG-148 recommendation in one quarter of the measurements. The introduction of the asymmetric FWs might require dosimetric evaluation similar to that from which the original 1% FWHM tolerance was established. Furthermore, the establishment of an appropriate QA tolerance for the asymmetric FWs becomes more relevant with the recent development of motion management utilizing the dynamic jaws. A next step should be to evaluate the clinical significance of the observed measurement deviations and reported discrepancies from current standard QA tolerance limits.

Replacing patient specific quality assurance measurements with log file based Monte Carlo simulations for proton therapy.

C. Winterhalter, G. Meier, E. Fura, A. Bolsi, A. Fredh, D. Oxley, D.C. Weber, S. Safai, A. Lomax

Centre for Proton Therapy, Paul Scherrer Institute, Villigen, Switzerland

Introduction

In proton therapy, patient specific quality assurance (PSQA) measurements are time consuming and limit the patient throughput. Additionally, they are not sensitive in picking up delivery errors and, as doses are verified in a water phantom, do not represent the patient geometry. As an alternative, here we investigate a log-file based Monte Carlo approach to PSQA.

Materials and Methods

Monte Carlo simulations of 104 fields in a water tank have been compared to PSQA measurements. Additionally, absolute dose factors have been predicted in the patient geometry based on log-file (information recorded during delivery) Monte Carlo simulations, which include both delivery and calculational uncertainties. Finally, the relative agreement between log-file Monte Carlo and analytical calculations has been analysed.

Results

After accounting for a 1% offset, for 94% of the fields absolute doses simulated in water fit measurements to within 2%, with a maximum difference of 2.3%. Normalization factors based on the log-file Monte Carlo simulations in the patient CT match to within 3% with measured absolute dose scaling factors. Relative dose distributions agree with analytical calculations to within 5 % for over 99% (paraspinal), 98% (skullbase), 97% (brain & nasal cavity), 90% (lung) of the voxels with dose >10% of the prescription dose.

Conclusion

A log-file based Monte Carlo simulation approach, which includes both delivery and calculational uncertainties and enables absolute dose predictions directly in the patient CT, has been demonstrated for proton therapy. As a replacement for patient specific verifications, this method could increase available beam time for patient treatments without jeopardizing the treatment quality.

Dosimetric implications of Geant4 version changes for proton radiation therapy

R. Kueng (1), E. Wall (2), D. Frei (1), P. Manser (1), M.F.M. Stampanoni (3), M.K. Fix (1)

(1) Division of Medical Radiation Physics and Department of Radiation Oncology, Inselspital, Bern University Hospital and University of Bern, Switzerland
(2) Department of Physics, Swiss Federal Institute of Technology ETH Zürich, Switzerland
(3) Institute for Biomedical Engineering, ETH Zürich and PSI, Villigen, Switzerland

Introduction
For proton radiation therapy, an accurate prediction of dose distributions is essential. In clinical as well as in research settings, various types proton dose calculation algorithms are in use. Dose calculation by means of Monte Carlo (MC) simulations is considered the gold standard for dose estimation, with the Geant4 toolkit being the most widely used MC transport code for protons in radiation therapy. The purpose of this work is to investigate the dosimetric impact of changing Geant4 version and electromagnetic physics option on resulting dose distributions.

Materials and Methods
Geant4 version 9.3.p01, 10.1.p03 and 10.4.p02 are used to calculate dose distributions of mono-energetic proton pencil beams in three different homogeneous phantoms (water, cortical bone and titanium). The standard electromagnetic physics list option 3 and option 4 are loaded to run the simulation in each Geant4 version. Differences in the resulting dose distributions are investigated by analyzing integrated depth dose curves and lateral dose profiles.

Results
Varying the Geant4 version for a fixed physics option shows substantial variation of the dose distributions, manifesting in differences in proton range of up to 0.5 mm (R50) and changing profile width of up to 1 mm (DTA at 10% D_{max} in Bragg peak). Discrepancies arise from underlying physics models, which can change for different versions even for fixed physics user settings. Additionally, changing the electromagnetic physics list from standard option 3 to standard option 4 for a fixed Geant4 version yields range differences of up to 0.1 mm (R50) and changing profile width of up to 0.5 mm (DTA at 10% D_{max} in Bragg peak).

Conclusion
Variation of software version and electromagnetic physics list was shown to substantially influence the dose distributions of mono-energetic proton pencil beams on homogeneous phantoms. Thorough validation of the MC dose calculation framework is crucial when changing versions and/or physics lists as the underlying implementation might change.

Spot and layer spacing optimization for proton pencil beam scanning with Eclipse TPS

N. Bizzocchi, M. Bobic, T. T. Böhlen, A. J. Lomax, J. Hrbacek

Proton Therapy Center, Paul Scherrer Institut, Switzerland

Introduction This summer the Paul Scherrer Institut's Proton Therapy Center opened the Varian ProBeam gantry for clinical operation. During the commissioning phase of the Eclipse Treatment Planning System (Version 13.7), sub-optimal dose homogeneity was observed on rectangular targets contoured in water phantoms. These include ripples in the dose distribution and severe under dosage in proximal parts of target volumes extending extensively in the beam direction. In this study, the dependency of dose homogeneity and conformity as a function of different layer-spacing (LS) and spot-spacing (SS) were investigated in order to mitigate these issues.

Materials and Methods The starting point of this study was the clinical machine settings used for Eclipse TPS commissioning. NUPO (Nonlinear Universal Proton Optimizer, Version 13.7.16) was used for plans optimization. 5 different rectangular targets contoured on a water phantom were tested using a single field: 3 of them were planned both with and without range shifter (RS), 1 with RS and 1 without, making a total of 8 different planning scenarios. Target margins for initial spots deposition were set to 0.5 cm at the proximal and distal end of the target, while the lateral margin was set to 1 cm. The prescribed dose was 0.5 Gy for each target except for the longest one (18 cm long) that was prescribed a dose of 1 Gy in order to compensate for under dosage due to the high minimum deliverable spot threshold (MDT). The use of a smaller LS than the clinical one (3.0 MeV instead of 3.5 MeV spacing step between contiguous layers), mitigated the dose ripples in the longitudinal direction. With this new LS configuration two machine options were then tested, *spot size in air* (SSA) -used for the TPS commissioning- and *spot size in water* (SSW). Both of these options were tested with 4 different SS factor, leading to a total of 64 SS combinations. The resulting dose distributions, as well as the total number of delivered spots per field, were compared with the clinical settings of the ProBeam system. Homogeneity Index (HI) D_5-D_{95}/D_p*100 was used for the dose distribution evaluation.

Results The attached table shows the results for the 72 tested scenarios. Using a smaller LS led to more spots per plan and increased issues with the MDT. These could however be compensated using a larger SS, leading to a decreased spot density up to 15% less than the default settings. It has to be assessed if the overall lower number of spots could affect the plan robustness. In general the SSW setting performed worse than the SSA one, the former introducing significant lateral edge dose enhancements which resulted in worse HI and target conformity. One reason could be that the SSW setting does not take in consideration the spot spreading when the RS is inserted, affecting the SS optimization.

Conclusion The tested settings achieved improved homogenous dose distribution in cases without the RS, while decreasing the total number of spots by ~ 15%. For SFUD plans using multiple fields with low dose per fraction, the new setting may present a viable solution to the TPS issues.

Is Monte Carlo planning really justified in intracranial radiosurgery?

Z. Girbau, N. Lomax, S. Alonso, G. Lutters, S. Bodis

Radiation Oncology Centre KSA-KSB, Kanton Spital Aarau, Aarau, Switzerland

Introduction

The Pencil Beam (PB) algorithm presents dose distribution calculation deficiencies for small cranial lesions close to bone or air cavities. The aim of this work was to investigate the value of using the Monte Carlo (MC) algorithm in such regions as it models better the scattering processes that occur in different density tissues. We present a comparison of different Radiosurgery (RS) intracranial plans computed with both algorithms.

Materials and Methods

Patients treated with RS for vestibular schwannoma and cranial metastasis and treated at our hospital have been randomly selected. We have calculated the delivered dose distributions with the Treatment Planning System (TPS) iPlan (RT Dose v.4.5.5., BrainLab, Feldkirchen, Germany) using both the MC and PB algorithms. Additionally, we have evaluated the performance of the MC algorithm for the dose calculation options: Dose-to-Medium (D_M) and Dose-to-Water (D_W).

Results

Table 1 contains the PTV (vestibular schwannoma) mean dose and coverage for three cases calculated with MC and PB and Fig.1. is an example (case I) of DVH for the PTV and cochlea (OAR).

Vestibular Schwannoma	Case I	Case II	Case III
PTV dose (Gy)			
Mean dose PB	14.5	13.7	14.2
Mean dose MC D_M	14.4	13.7	14.4
Mean dose MC D_W	14.6	14.4	15.3
% Difference PB vs MC D_M	0.8	0.1	-1.3
% Difference PB vs MC D_W	-0.6	-4.9	-7.5
% Difference MC D_M vs. D_W	-1.3%	-4.8%	-5.8%
PTV coverage (%)			
Coverage PB	99.2	98.5	98.1
Coverage MC D_M	98.7	96.3	97.2
Coverage MC D_W	99.0	99.0	98.4

Table 1.

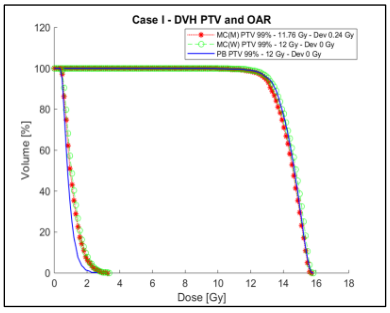

Figure 1.

Conclusion

The use of MC may be justified in intracranial RS planning in order to give a more accurate representation of the dose delivered to lesions surrounded by bone and air cavities, as well as for the OARs, but for the majority of cases located in homogeneous regions PB and MC show a mean dose difference within 1.8 ± 0.002% and PB may be considered satisfactory.

Beam monitoring through out-of-field measurements in a pulsed electron beam at ultra-high dose-rate

P. Gonçalves Jorge (1), C. Bailat (1), MC. Vozenin (2,3), J. Bourhis (2), F. Bochud (1), R. Moeckli (1).

(1) Institute of Radiation Physics (IRA), Lausanne University Hospital, Lausanne, Switzerland
(2) Department of Radiation Oncology, Lausanne University Hospital, Lausanne, Switzerland
(3) Radio-oncology Laboratory, Lausanne University Hospital, Lausanne, Switzerland

Introduction

Published studies concerning radiotherapy at ultra-high dose-rate (FLASH) showed an increase in the differential response between normal and tumor tissues compared to conventional radiotherapy. For FLASH radiotherapy, conventional monitor chambers are unable to collect all the charges created by the ionizing radiation, leading to saturation. This is why the development of monitoring tools for high dose-rate beams is important for pre-clinical studies.

Materials and Methods

The monitoring system was composed of an Advanced Markus ionization chamber (corrected for ion recombination) that was positioned out-of-field at the exit of beam. A second Advanced Markus ionization chamber (corrected for ion recombination) was placed in the center of the field as for usual dose measurements. The dose measured by both ionization chambers was recorded and their ratio was calculated. These measurements were made by using different configurations (dose-rate, number of pulses, etc…)

Results

Relations between scattered dose and beam parameters were studied. For example, a linear relation between the pulse repetition frequency and the scattered dose was found. The presence of backscattered dose was detected by the out-of-field ionization chamber for SSD smaller than 10 cm with an increase in dose that remained below 2%. For each given configuration (fixed parameters), the ratio of doses was repeatable in time within 1% uncertainty.

Conclusion

This study showed that an ionization chamber placed out-of-field is a possible way to monitor the dose of the primary beam. Additionally, the scattered dose is dependent on the beam parameters.

Quality assurance of small animal irradiation: validation of a 3D-printed phantom for delivered dose evaluation

Nikolaos Koutsouvelis (1), Giovanna Dipasquale (1), Michel Rouzaud (1), Angele Dubouloz(1), Philippe Nouet (1), Maud Jaccard (1), GARIBOTTO Valentina (3), TOURNIER Benjamin B (4), Thomas Zilli (1,2)

(1) Department of Radiation Oncology, Geneva University Hospital, Geneva, Switzerland;
(2) Faculty of Medicine, Geneva University, Geneva, Switzerland;
(3) Department of nuclear medicine, Geneva University Hospital;
(4) Division of Adult Psychiatry, Department of Mental Health and Psychiatry, University Hospital of Geneva;

Introduction
In this study, we report on the use of a 3D-printed rat phantom for radiotherapy dosimetric “quasi-in vivo” quality assurance for small animal irradiation.

Materials and Methods
We aimed to irradiate with a dose of 2 Gy per fraction the half-brain of a rat model. The dose was delivered by a 4 MV X-ray beam using a direct anterior-posterior, hemi-field beam, with a size of 3cm x 4cm. A 2cm thick 3D-printed bolus made of poly lactic acid (PLA) was used to avoid the build-up region of the beam in the target volume. To verify proper dose delivery, a 3D 1:1 scale printed copy of the rat body was produced from the CT dataset of the rat to be used as a phantom for dose measurements. Thermoluminescent dosimeters (TLDs) and gafchromic films, to analyze profile within the brain, were used.

Results
Gafchromic film dosimetry showed a good concordance between the planned dose distribution and the measured dose. Mean TLDs percentage dose differences, were 1.3% in-field and 0.9% beneath bolus. Out of field, dose measurements gave a mean of 0.05Gy for an expected dose of 0.04Gy.

Conclusion
A 3D-printed 1:1 scale rat phantom is an effective and reliable tool for “quasi in-vivo” dosimetric quality assurance in the setting of small animal radiotherapy research.

Abstracts – Oral presentations

Session Nuclear Medicine, radiation protection, radiation metrology & radiobiology

Phantom-based image quality assessment and clinical protocol optimization in SiPM PET/CT and comparison with conventional PMT-based PET/CT devices

C. Kieffer(1), TVM.Lima(2), F.R. Verdun(1), J-P. Papazyan(3), K. Zeimpekis(4), R. Guignard(5), J.O. Prior(6), S. Gnesin(1),

(1)Institute of Radiation physics, CHUV, Switzerland
(2)Radiation Protection Group, Kantonsspital Aarau, Switzerland
(3)Radiology and medicine nuclear department, Genolier Clinique, Switzerland
(4)Department of nuclear medicine, Zürich UniversitätsSpital, Switzerland
(5)Department of nuclear medicine, Hopital de La Tour, Switzerland
(6)Department of nuclear medicine and molecular imaging, CHUV, Switzerland

Introduction

The purpose of this study was to investigate the image quality achievable in three different, state-of-the-art SiPM TOF PET/CT and compare with a conventional PMT-based PET/CT devices. Furthermore we assessed clinical 18F-FDG oncologic PET protocols to identify margins for optimization and optimal trade-off between administered activity (patient dose exposure/signal-to-noise ratio) and acquisition time (patient comfort/spatial resolution) while preserving diagnostic information.

Materials and Methods

We performed 300s list-mode (LM) PET acquisitions of a NEMA/IEC NU2 phantom, with activity concentrations of 5kBq/mL and 25kBq/mL for the background (9.5L) and sphere inserts respectively. Adopting the local clinical protocol setup, in each device, reconstructions were obtained varying the image statistics (10, 30, 60, 90, 120 and 180s from LM data) and the number of iterations (1 to 10). Quantitative cross-calibration, image noise on the uniform background assessed by the coefficient of variation (COV), recovery coefficients (RCs) evaluated in hot spheres and a cold contrast (in a lung insert) were evaluated per each reconstructed dataset. The characteristic scan time × mass-activity administered (TAP) was compared among datasets.

Results

Good system cross-calibration was obtained for all tested dataset with <10% deviation from the expected value was observed. For all clinical protocol setups, image noise was compatible with clinical interpretation (COV<15%). SiPM-based PET evidenced improved signal-to-noise compared to conventional PMT-based PET. RCs were comparable between SiPM-based and PMT-based PET datasets. RCs from SiPM-based PET were less noise-sensitive. SiPM-based PET provided comparable image quality with lower TAP (~30% less) compared to PMT-based PET.

Conclusion

This study compared the image quality achievable in clinic in three state-of-the-art SiPM PET/CT devices (from all possible vendors [N=3]) as well as image quality obtained in a conventional SiPM-based PET. Reported results show that a comparable image quality is achievable with a TAP reduction of ~30% in SiPM-based PET. This could lead to a significant reduction of the mass-activity administered and/or scan time with direct benefits in terms of dose exposure, image quality and patient comfort.

Deep Learning for the Detection of Lesions on ^{68}Ga-PSMA PET/CT Imaging

Kuangyu Shi (1,2), Yu Zhao (2), Lina Xu (2), Giles Tetteh (2), Andrei Gafita (3), Fabian Haupt (1), Ali Afshar-Oromieh (1), Matthias Eiber (3), Bjoern H Menze (2), Axel Rominger (1)

(1) Dept. Nuclear Medicine, University of Bern, Switzerland
(2) Dept. Computer Science, Technical University of Munich, Germany
(3) Dept. Nuclear Medicine, Technical University of Munich, Germany

Introduction

The emerging PSMA targeted radionuclide therapy provides an effective method for the treatment of advanced metastatic prostate cancer. To optimize the therapy effect and maximize the theranostic benefit, it is urgently needed to characterize all the lesions to target before the treatment. However, this is extremely challenging considering the factor that dozens of lesions of heterogenous size and uptake may distribute in a variety of anatomical context with different background. Until now, there is no successful computer-aided lesion detection methods for PSMA imaging.

Materials and Methods

A starting cohort of 71 patients (46 from LMU, 5 from Bern, 20 from TUM) with advanced metastatic prostate cancer were scanned with ^{68}Ga-PSMA-11 PET/CT. For proof-of-concept, we focus on the detection and segmentation of bone & lymphnode lesions in pelvic area. A multi-task deep learning architecture based on fully convolutional neural networks was developed to detect the lesions. It extracts salient features from PET and CT first and then combines these features to automatically detect the lesions. The framework contains five fully connected convolutional layers and two sigmoid classification layers. For comparison, the detection accuracy of conventional W-Net (cascaded V-Nets) were calculated.

Results

Compared with conventional W-Net, the multi-task deep learning has improved the detection rate of bone lesion from 82.6% to 88.9%. The detection rate of lymph node lesions is still limited due to the restricted number of lesions (n=63) available. Nevertheless, the multi-task deep learning has improved the detection rate of lymphnode lesions from 66.4% to 72.5%.

Conclusion

We proposed the first deep learning method for automatic detection of lesions on ^{68}Ga-PSMA-11 PET/CT images. A multi-task deep learning method was developed to improve the detection accuracy compared with conventional W-Net. The preliminary test on pelvic area confirmed the potential of deep learning methods. At the moment, more data are collecting in Bern and TUM. Increasing the amount of training data may further enhance the performance of the developed deep learning methods.

Optimization of alanine dosimetry for doses from 10Gy to 100Gy for flash-beam radiotherapy

Maude Gondré (1), Patrik Jorge (1), Claude Bailat (1), Marie-Catherine Vozenin (2), Jean Bourhis (2), François Bochud (1), Raphaël Moeckli (1)

(1) Institute of Radiation Physics, CHUV, Lausanne
(2) Department of Radio-Oncology, CHUV, Lausanne

Introduction

Alanine dosimetry relies on the principle of electron paramagnetic resonance spectroscopy (EPR). The irradiation of an alanine pellet creates stable radicals in proportion with the dose. The dose is then determined by measuring the absorption to higher energetic level of unpaired electrons shined by a specific resonant frequency and within a variable magnetic field. The measurement process to achieve high accuracy can be time consuming, especially for low doses such as 10 Gy, and many lecture parameters can influence the final reading. Therefore, each parameter has to be optimally defined in order to achieve the highest signal-to-noise (SNR) ratio while limiting the time of lecture.

Materials and Methods

For the optimization of the lecture parameters, the Bruker e-scan EPR spectrometer and calibrated alanine pellets of 10Gy to 100Gy provided by Bruker have been used. The EPR spectrum have been recorded using the WinAcq application of the e-scan program, that allows modifying the Bruker default acquisition parameters such as the conversion time, the number of scans, the time constant or the amplitude of modulation of the magnetic field. The first two parameters allow the optimization of the lecture time while the amplitude modulation and the time constant influence the SNR. Therefore, these parameters were the key to reduce the time without losing a large fraction of the amplitude signal.

Results

By reducing the number of scans by a factor of 4.47 and increasing the time constant from 5.12ms to 20.48ms and the gain from 100 to 1950, the time of scan could be reduced from 5.58 minutes to 2.61 minutes, while maintaining a similar SNR. Finally, low doses such as 10Gy could be measured by performing 3 rounds of lecture, leading the total time of lecture to 10.5 minutes, with a relative difference less than ±2%.

Conclusion

By optimizing the lecture parameters of the EPR spectrometer, measurement of low doses can be achieved within an acceptable time and good accuracy.

FLASH Radiotherapy: Spare the normal tissue but not the tumor by oxygen-dependent mechanisms.

P. Montay-Gruel (1), K. Petersson (1), J. Ollivier (1), B. Petit (1), P. Jorge Goncalves (1), (2), F Bochud (2), J-F. Germond (2), P. Froidevaux (2), R. Moeckli (2), C. Bailat (2), J. Bourhis (1), and M-C. Vozenin (1)

(1) Department of Radiation Oncology/DO/Radio-Oncology/CHUV, Lausanne University Hospital, Switzerland.
(2) Institute of Applied Radiation Physics/CHUV, Lausanne University Hospital, Switzerland.

Introduction

Despite important technological advance and dose delivery precision, radiation-therapy still induces irreversible side effects, justifying the urge to develop new radiation-therapy techniques. Preclinical studies on FLASH irradiation (FLASH-RT) showed a possibility to efficiently treat the tumors, without inducing drastic side-effects on the normal tissue, by increasing the dose rate over 100 Gy/s. This so called FLASH-effect has been identified as oxygen-dependent and opens new possibilities in the radiation therapy field.

Materials and Methods

The effects of FLASH-RT on the tumor and on the normal tissue have been studied on murine glioblastoma models and healthy animal models irradiated with a LINAC prototype eRT6 (PMB-Alcen) available at the CHUV. This experimental device delivers a pulsed electron beam at both conventional (0.1 Gy/s) and FLASH (>100Gy/s) dose-rates with an adequate and precise dosimetry. The biological response was evaluated post-irradiation. The production of hydrogen peroxide in water irradiated with conventional dose-rate versus FLASH-RT was measured to complete the biological results obtained in hyperoxic and hypoxic tissues.

Results

Our results show that conventional dose-rate and FLASH-RT trigger a similar anti-tumor effect on a glioblastoma model. Nevertheless, for a similar dose, FLASH-RT induces no large cellular or functional toxicity compared to conventional dose-rate RT. Interestingly, this protection was reversed by an increase in oxygen tension in the tissue, suggesting an oxygen-dependent protective mechanism. Moreover, the measurement of hydrogen peroxide production in irradiated water showed that FLASH-RT induces less production of H_2O_2 than conventional dose-rate at isodose.

Conclusion

On all studied models, we showed that FLASH-RT does not induce normal tissue damage while triggering a similar anti-tumor effect compared to conventional dose-rate irradiation. Investigation of FLASH-RT effects on hypoxic and hyperoxic tissues along with radio chemistry results suggest an oxygen-dependent mechanism responsible for less oxidative stress production and explaining the normal tissue sparing.

HOW AND WHY IS THE MEDICAL PHYSICIST UNIT OF RADIOPROTECTION USEFUL IN A RADIOLOGY DEPARTMENT? A QUANTITATIVE ANALYSIS

L.Bellesi(1), D.Gaudino(1), F.Pupillo(1), M. A. Piliero(1), M. Casiraghi(1) and S. Presilla(1).

(1) Ente Ospedaliero Cantonale, Servizio di Fisica Medica, Ospedale San Giovanni Bellinzona, Svizzera

Introduction

Contributions of a Clinical Medical Physics unit of radioprotection (CMPu) are given essentially in the field of patient dose monitoring, assessment of staff occupational exposure, quality assurance programs, education, medical research and economics. The purpose of this article is to describe quantitatively the effects of the CMPu engagement in the radiology department on dose and image quality indexes. Data from different devices installed in four RDs of a multicentre hospital were analysed.

Materials and Methods

Dosimetric and image quality data from C-arms, Mammography and CT systems were collected from all imaging modalities in all Hospitals. Statistical indexes were extracted from a data collection software, from PACS or directly from the devices.

Results

Data showed that dose and image quality optimization could not be obtained only introducing new hardware or software technology. Doses from CT modalities were considerably reduced thanks to the work carried out by the CMPu together with the technologists, nurses and physicians of the RD. DLP for Thorax and Chest CT exams had an average decrease of about 36% from 2015 to 2018. C-Arms imaging showed initially high dose levels due to incorrect implementation of protocols. After the collaboration between CMPu, RD and surgery staff, C-Arms doses were reduced by 37% in term of average DAP from 2017 to 2018. On the other hand, the implementation of a newer mammographic system in all hospitals, resulted in a general mean glandular dose increase of about 38.3% from 2017 to 2018, probably due to a lack of a protocol optimization strategy.

Conclusion

Strategies for dose reduction and optimization of imaging protocols must be planned with the CMPu in order to obtain good results in terms of balance between image quality and patient dose especially when a new technology is introduced. The scheduling of team meetings is essential to share knowledge and organize activities related to optimization of exams.

Abstracts – Oral presentations

Session Radiological Physics I

Diagnosis of crystal-related arthropathies with a multi-energy spectral photon counting CT

Anaïs Viry (1), Aamir Raja (2), Lisa Stamp (3), Francis R. Verdun (1), Fabio Becce (4)

(1) Institute of Radiation Physics, Lausanne University Hospital, Lausanne, Switzerland
(2) Department of Radiology, University of Otago, Christchurch, New Zealand
(3) Department of Rheumatology, Immunology and Allergy, University of Otago, Christchurch, New Zealand
(4) Department of Diagnostic and Interventional Radiology, Lausanne University Hospital, Lausanne, Switzerland

Introduction

Crystal-related arthropathies are joints disorders characterized by an accumulation of crystals in joints. Different types of crystals can be involved, monosodium urate (MSU), basic calcium phosphate (with hydroxyapatite HAP and octacalcium phosphate OCP) and calcium pyrophosphate (CPP). Their identification is very important for diagnosis and management of the disease (by assessing the treatment response). The goal of this study will be to assess spectral photon counting CT (SPCCT) diagnostic performances for the discrimination between crystals in vitro and ex-vivo

Materials and Methods

A calibration phantom composed with the various crystal samples was scanned using a SPCCT protocol for bone imaging. Images were reconstructed using 4 energy bins 20-30 keV, 30-40 keV, 40-50 keV and 50-80 keV. A linear discriminant analysis was performed to find a linear combination between energy bins which maximize the discrimination between the crystals. Accuracy was used as a figure of merit to assess the discrimination between two crystals. Then, two excised human specimens, presenting clinical signs of different arthropathies were scanned using the same SPCCT protocol. Images of specimens were calibrated using mass attenuation coefficients from the calibration phantom and reconstructed with a material decomposition algorithm.

Results

In-vitro results shows that MSU can be accurately differentiated from CHA and CPP (accuracy 99%) then CPP can be moderately discriminate from CHA (accuracy 84.1%). Ex-vivo results shows that SPPCT can correctly identify MSU, CPP and CHA in human specimens.

Conclusion

Multi-energy SPCCT can differentiate in vitro and ex-vivo MSU, CHA and CPP. Further studies will determine whether these promising preliminary results will hold true in vivo.

Clinical impact of CT protocol optimisation in adaptive radiotherapy

Thiago VM Lima (1), Ismail Oezden (1), Christian Sommer (2), Mauricio Leick (3), Sara Alonso (3), Joerg Binder (1), Stephan Scheidegger (2), Gerd Lutters (1,3)

(1) Fachstelle Strahlenschutz, Kantonsspital Aarau, Switzerland
(2) ZHAW School of Engineering, Winterthur, Switzerland
(3) Radiation Onkologie, Kantonsspital Aarau, Switzerland

Introduction

The goal of an adaptive radiotherapy is to compensate to the changes in the applied dose distribution caused by the occurring geometrical and pathological variations throughout the course of the patient's treatment. Although most common clinical protocols include multiple image modalities for the initial treatment planning, along the treatment, CT is kept as the main source of imaging performed in the patients. The aim of this work is to evaluate and optimize radiotherapy clinical CT protocols for the detection of small lesions and assess the clinical impact of this optimisation.

Materials and Methods

A low contrast detectability phantom [1] based on difference detail curve (DDC) [2] has been developed by the ZHAW and it was used. The phantom consist on a cylindrical DDC insert with low contrast objects representing native and contrast enhanced structures, which has been used in combination with an elliptical PMMA phantom with an effective diameter of 32 cm (equivalent to a human body) and an anthropomorphic head phantom. The phantoms were scanned with the current clinical protocol and compared to a DDC characterization catalogue based on several measurements from multiple devices. As part of the DDC analysis several human observers performed the DDC evaluation of the acquired images on a clinical medical grade display located in a room with controlled light conditions.

Results

A logarithmic fit was applied to the measured DDC data (a+b.log (x)) for the tested protocol. The fitted DDC was compared to benchmark results from other 120 measurements in over 14 devices with similar protocol parameters within our catalogue of measurements.

Conclusion

The DDC has previously been shown to be a suitable method for protocol optimisation in relation of dose and image quality [1]. From the benchmark of the clinical abdominal protocol against a catalogue of measurements we were able to show that is possible to further improve small lesion detectability especially for lesions below 7 mm diameter.

References

[1] Sommer et al, Suitability of Difference Detail Curve for Image Quality and Inter-Observer Variability, SSBE Annual Meeting 2018
[2] Sommer et al, Current Directions in Biomedical Engineering, 3(2):517-519, 2017.

Optimization of abdominal CT protocols using a model observer: a multi-centric quantitative analysis

D. Racine (1), N. Ryckx (1), A. Viry (1), F. R. Verdun (1)

(1) Institute of Radiation Physics – Lausanne University Hospital, Rue du Grand-Pré 1 – 1007 Lausanne – Switzerland

Introduction

(1) To highlight the variation of patient exposure and image quality performances for various abdominal protocols. (2) To create an optimization scheme for each abdominal protocol.

Materials and Methods

An anthropomorphic abdominal phantom (QRM, Moehrendorf, Germany) with an optional ring, representing the attenuation of an adult abdomen of 75 kg (medium phantom), was scanned on 68 CT machines in the Western part of Switzerland. Firstly, the phantom was scanned with the dose obtained using the local clinical settings of the portal phase for the detection of focal liver lesions (FLL). Secondly, the local clinical settings were changed to obtain a $CTDI_{vol}$ of about 20 % lower and higher than the locally obtained $CTDI_{vol}$. Finally, the phantom was scanned with a maximum $CTDI_{vol}$ equal to 20 mGy. For statistical reasons, the phantom was systematically scanned 8 times at each dose level. To evaluate the low contrast detectability (LCD), 88 regions of interest (ROIs) including spheres of 6 mm in diameter with a contrast of -20 HU relative to the background at 120 kV and 300 ROIs with background noise were used. LCD was objectively assessed on theses ROIs with a Channelized Hotelling mathematical model Observer (CHO) with ten dense differences of Gaussian channels using a Receiver Operating Characteristic (ROC) paradigm. The area under the ROC curve (AUC) was used as the figure of merit (FOM) for the image quality and the displayed $CTDI_{vol}$ was used as FOM for patient exposure.

Results

The median $CTDI_{vol}$ obtained using the local clinical settings of the portal phase for the detection of FLL was 11.6mGy (interquartile range (IQR) = 4.9mGy) and the median AUC was 0.84 (IQR = 0.05).

Conclusion

A comparable image quality cannot be reached on different scanners facilities at the same dose level. Therefore, the image quality requirements, related to the clinical question to be answered, should be the starting point of patient dose optimization.

Update of the Diagnostic Reference Levels for CT in Switzerland with Dose Management Software

Christoph Aberle (1), Reto Treier (2), Sebastian Schindera (3)

(1) Department of Radiology, University Hospital Basel, Basel, Switzerland
(2) Radiation Protection Division, Federal Office of Public Health, Bern, Switzerland
(3) Department of Radiology, Kantonsspital Aarau, Aarau, Switzerland

Introduction
The previous Swiss national diagnostic reference levels (DRLs) for CT were established in 2010. As a result of this work, they were updated in 2018 by acquiring big data on CT radiation doses with dose management software.

Materials and Methods
The CT dose data from 14 radiological institutes in Switzerland with a total of 50 CT scanners were collected with locally installed dose management software solutions between 2014 and 2017. The data were subdivided in 15 different standard CT protocols. Data cleaning steps were developed and adjusted individually for each participating institute and protocol. After data cleaning, 220‘269 CT exams were available. The DRLs were calculated as the 75th percentile of median $CTDI_{vol}$ and DLP values per scanner. They were compared to the previous national DRLs published in 2010.

Results
Compared to the old DRLs, a clear trend towards lower doses is observed. The average relative change in $CTDI_{vol}$ was -30% (0% to -47% depending on the protocol) and -22% for DLP (+20% to -40%). The largest relative decrease in the DLP values was observed for the two neck protocols (standard neck, -32%, and carotid angiography, -28%), the two chest protocols (standard chest, -37%, and exclusion of pulmonary embolism, -33%) and the cervical spine protocol (-40%). The DRLs for other protocols, for example the standard head and the standard abdomen-pelvis protocol, showed smaller relative changes (-11% and -17%).

Conclusion
The updated national DRLs for CT are substantially lower compared to the previous DRLs, demonstrating the efforts of the radiological community to lower CT radiation exposure.

Swiss National CT Dose Registry

Thiago VM Lima (1), Daniel Sigrist (2),Sebastian Schindera (2)

(1) Fachstelle Strahlenschutz, Kantonsspital Aarau
(2) Institüt für Radiologie, Kantonsspital Aarau

Introduction

At the current time, approximately 255 institutes in Switzerland are equipped with at least one CT scanner, resulting in a combined total of over a million CT exams per year. While individual dose information is stored in a picture archiving and communication system (PACS) on a per-exam basis, systematic and comprehensive analysis usually requires high manual effort. However, such an analysis of patient exposure is inevitable for quality assurance and improvements in radiological processes. A national dose registry aims to serve as a central platform to collect, analyse and publish dose information from different radiology institutes across Switzerland for benchmarking and optimizing the exposure of various CT protocols. The aim of this work is to share how this platform is being developed, current status and next steps.

Materials and Methods

Building a national dose registry requires the collaboration and participation of many institutes equipped with dose management system (DMS). A primary requirement for participating institutes is the utilisation of a DMS so that initial data collection and processing can be performed locally. Data submission is designed as a semi-automatic process, thus minimising the recurring effort of participating institutes and fostering a larger and more up-to-date data corpus.
Currently, a feasibility study is being carried out. It is concerned with strategical topics such as financing and operations, but also entails the definition of processes and the development of a proof-of-concept web platform. During the feasibility study, a few early adopter radiological institutes are going to be connected.

Results

Technical aspects of the server, data structure and transfer preferences have been set from collaboration with major DMS vendors. A web-platform with basic analysis and reporting tools have been designed and deployed with previous available patient exposure data. Validation steps are currently being designed and extended.

Conclusion

The Swiss National CT Dose Registry project aims to semi-automatically collect, aggregate and analyse CT radiation dose data from Swiss radiology institutes. A central platform is created which allows the exchange, publication and review of analyses based on a broad and up-to-date data corpus. Gained insights can then be utilised for quality assurance and process optimisation in radiology institutes, allow more frequently updated diagnostic reference levels, aid in protocol optimisation and may indirectly lead to patient dose reduction.

Abstracts – Oral presentations

Session Radiological Physics II

Machine Learning based Feature Detection on 2D X-Ray Images

Toon Roggen, Stefan Scheib

Varian Medical Systems, Imaging Laboratory

Introduction

Radiotherapy treatments relying on gating or in-treatment position verification, favor the use of metallic fiducials implanted close to the target. These metallic fiducials are visualized on kV triggered images, acquired with an on-board kV imager. The drawbacks of metallic fiducials are apparent and the use of anatomical structures (bone, soft tissue) as alternative landmarks would significantly facilitate the choice for gating or in-treatment position verification. The latest advances in machine learning enable pursuing this approach.

Materials and Methods

As a suitable implementation for in-treatment landmark detection on kV triggered images, Mask R-CNN was identified. This R-CNN (Regional Convolutional Neural Network) provides a segmentation mask and a bounding box for the detected object, and is based on a Feature Pyramid Network (FPN) and a ResNet101 backbone. An implementation was done in Python 3, with Keras, and a TensorFlow back-end. The training, validation and test data was curated and annotated semi-automatically from projection images of the abdominal region of a patient with implanted fiducials. For each fraction 850 projection images of the abdomen were taken with the intent to reconstruct a CBCT (Cone Beam Computed Tomography). As CNNs require a vast amount of training data and the image quality is comparable with triggered images, these projection images serve as an excellent training set.

Results

The combined model differentiates between the following categories: stents, fiducial markers and vertebrae. It can distinguish between different objects of the same category, which allows for position verification on the projection image. Mean Average Precision (mAP) at Intersection over Union (IoU) of 0.5, 0.75 and [0.5:0.05:0.95] are 72.9, 25.8 and 33.6.

Conclusion

A Mask R-CNN implementation was deployed and trained on kV projection images acquired with an on-board kV imager. The model detects stents, metallic markers and vertebrae in the abdomen. It is capable of distinguishing between different objects of the same category. The mAP rating of this first model encourages to continue developing this model further.

Why is it important to connect all X-ray units to a dose management system?

Elina Samara(1)

(1) Valais hospital

Introduction

According to the Swiss legislation, radiation dose needs to be registered for high- and medium-dose examinations. Radiation data are usually captured as images and stored in PACS. Dose management systems (DMS) are getting more and more popular as they offer not only the possibility to register the dose but also to provide a more thorough analysis. However, there are many practical difficulties when it comes to the connection of the DMS with X-ray units used outside the radiology department. This work aims to illustrate through a specific example the need to connect all radiological devices to a DMS.

Materials and Methods

The DMS that was recently installed in the hospital receives information from examinations performed in the radiology department. Image files for procedures performed in the operating theater are usually controlled by a radiographer before being manually sent to PACS for errors in patient ID, etc. and up to now, they are not forwarded to the DMS.

A severely injured patient received 15 radiological examinations in a six-day period. Seven of these were radiographies and five were CT. The patient underwent three operations under fluoroscopy guidance in the operating theater. During the regular file control, a radiographer noticed that the patient received an unusually high radiation dose and contacted the medical physicist to share her concerns. Effective and skin dose from all examinations had to be calculated manually and the results were communicated to the physicians for the patient follow-up.

Results

This case demonstrated that we could easily miss high patient irradiation with potential tissue reactions due to technical difficulties. The absence of a RIS for the operating theater complicates data collection and verification. Mobile X-ray units that are widely used in the operating theatre have lower standards in terms of connectivity and data transfer than those used in radiology departments. Radiation data saved in PACS contain limited information on radiation exposure.

Conclusion

More attention needs to be paid to the radiation use outside the radiology department. Although cases with multiple examinations and high doses are uncommon in diagnostic radiology, this example demonstrates that a DMS system that collects information from all devices is important for patient follow-up.

Dosimetric evaluation of the O-arm® imaging system

Pitteloud N[1,2], Sans Merce M[2,3], Damet J[2,4], Gamulin A[5], Lascombes P[6,7], Prod'homme M[6,7]

(1) Physics Section, University of Geneva, Geneva, Switzerland.
(2) Institute of Radiation Physics, Lausanne University Hospital, Lausanne, Switzerland.
(3) Division of Radiology, Geneva University Hospital, Geneva, Switzerland
(4) Department of Radiology, University of Otago, Christchurch, New Zealand
(5) Division of Orthopaedic and Trauma Surgery, Geneva University Hospital, Switzerland.
(6) Medical University of Geneva, Geneva, Switzerland
(7) Division of Paediatric Orthopaedic, Geneva University Hospital, Geneva, Switzerland

Introduction

Three-dimensional (3D) imaging devices are emerging in operating theatres for intra-operative applications. Although there are reported benefits of this technology, such as increased surgical accuracy and higher patient safety, radiation exposure of staff and patient remains a concern. This study aims at evaluating this exposure when using the O-arm® (2D and 3D imaging device).

Materials and Methods

To assess patient radiation exposure, absorbed doses to organs were measured on two anthropomorphic phantoms representing a five-year-old child and an adult female. The phantoms are made of slabs containing holes at the location of different organs, where thermoluminescent detectors (TLDs) were placed. Organ doses were measured for one 3D-aquisition of the O-arm® and during one minute of fluoroscopy using a conventional C-arm for comparative purposes. Skin entrance dose rates were also evaluated during 2D fluoroscopy by measuring incident kerma rates on the phantom. Staff exposure was evaluated by creating a 2D ambient equivalent dose cartography of the operating theatre for a single 3D O-arm® acquisition. Moreover, whole body and eye lens doses to the O-arm® technician were measured by placing an anthropomorphic phantom equipped with TLDs.

Results

Phantom organ doses for one 3D pelvic acquisition with the O-arm® ranged from 4.0 µGy to 6.7 mGy for the adult and from 0.9 µGy to 1.7 mGy for the child; on average 4 times higher than doses obtained after one minute of fluoroscopy with the C-Arm. Consistently, kerma rates at the surface of the skin were between 6 and 164 times lower for the C-Arm compared to the O-arm®. Results from the cartography showed that at 2 m from the isocenter, the maximum ambient equivalent dose is 11 µSv per acquisition and 3 µSv at the technician's position. Dosimeters placed on the technician phantom showed doses below the detection limit (i.e. 0.1mSv).

Conclusion

Doses delivered to the patient during a 3D acquisition of the O-Arm® are systematically higher than the corresponding irradiation with the C-arm. The staff, if positioned as far as possible from the isocenter and adequately equipped with protective gear, may remain inside the operative room during an O-arm® 3D acquisition.

Assessment of the efficiency in eye and brain dose reduction of a leaded facemask in clinical conditions using an anthropomorphic phantom and TLD

Nick Ryckx, Francis R. Verdun (1)

(1) Institute of Radiation Physics, Lausanne University Hospital, Switzerland

Introduction

In the last years, alarm has been rising within the interventional cardiology community because of increasing cases of cataracts among physicians. In addition, the publication of some case studies of brain tumors diagnosed within this collective has largely contributed to grow the unease, however there is, so far, no epidemiological evidence linking brain tumor to occupational exposure. Several vendors have proposed leaded facemasks, aimed at simultaneously reducing eye lens and brain exposure. This study aims at evaluating the dose reduction potential of such a device for both aforementioned organs.

Materials and Methods

To simulate the physician, we used the male adult Alderson-Rando phantom. The patient was simulated with a 30 x 30 x 20 cm PMMA stack. The angiography unit was placed in right anterior oblique (RAO) 45°, with the operator positioned next to the phantom as for a right femoral approach on a supine patient. The operator phantom was equipped with 44 TLD: 36 were distributed across the brain, two on each eye, two on each side of the thyroid, two on each side of the chest, and two for background measurement. The operator was also equipped with two electronic dosimeters at chest level. The PMMA was irradiated using the standard vascular protocol. The measurement was performed twice: once with the facemask on the phantom, once without. One TLD set was used for each measurement run.

Results

Both electronic dosimeters, as well as the angiography unit's acquisition parameters, indicated no significant changes in beam quality across both measurement sets. The reduction in eye lens exposure was respectively 65 and 51% for the left and right eye. The average dose reduction on the brain volume was 34%, the effect being more pronounced at the top of the brain (44% dose reduction) than the cerebellum (13% dose reduction).

Conclusion

Due to its geometry (high coverage of the face), a leaded facemask can serve as a handy tool for staff eye lens and brain exposure reduction. However, its efficiency is lower than that of other means of protection, such as leaded acrylic screens due to its low lead equivalent thickness (0.1 mm). It should therefore be used as a secondary tool, along with other means of protection. Limitations of the study include a fixed geometry (one operator head position, one beam angle) and a single beam quality.

Abstracts – Oral presentations

Session Radiotherapy II

CT lymph node radiomics improves prediction of locoregional control in head and neck cancer

Marta Bogowicz (1), Oliver Riesterer (1), Gabriela Studer (1), Jan Unkelbach (1), Christina Schröder (1), Matthias Guckenberger (1), Stephanie Tanadini-Lang (1)

(1) Department of Radiation Oncology, University Hospital Zurich, University of Zurich, Zurich, Switzerland

Introduction

Radiomics has been shown a promising tool for outcome prediction. So far radiomics-based models showed higher performance for endpoints related to the primary tumor rather than composite endpoints such as locoregional control (LRC) or overall survival. Most of the radiomics studies are based on the analysis of the primary tumor (PT) only. Here we hypothesize that LRC can be better predicted by a combination of PT radiomics and lymph nodes (LN) radiomics.

Materials and Methods

Head and neck squamous cell carcinoma patients treated with definitive radiochemotherapy were included in the retrospective study (training n = 77, validation n = 51). Radiomics analysis was performed on contrast-enhanced CT using Z-Rad implementation. 285 features were extracted from both PT and involved LN. The maximum relevance minimum redundancy method was used for selection of non-redundant features. The final model was trained using least absolute shrinkage and selection operator (100 times 10-fold cross validated).
Two models were trained. The first model (PT model) was based only on the PT radiomic features. In the second model (mixed model), the PT radiomics was first linked to local tumor control and the predictions obtained from this model were used as an input to LRC model together with LN radiomics. The performance of the models was tested in the validation cohort using the Wilcoxon test ($p < 0.05$) and the bootstrap method with 100 randomly selected samples to calculate the CI distribution.

Results

The PT model comprised 3 radiomic features. The mixed model used 3 PT radiomic features, as a preliminary prediction, and 4 LN radiomic features (mostly shape-based). Both models were significantly associated with LRC in the analyzed cohorts ($CI_{training\_PT} = 0.67$, $CI_{validaton\_PT} = 0.63$, $CI_{training\_mixed} = 0.75$, $CI_{validaton\_mixed} = 0.67$). The mixed model showed significantly higher performance than the PT model ($p < 0.01$). In the combination of PT radiomics and clinical nodal status for prediction of LRC, the nodal status was not a significant predictor.

Conclusion

This study shows that radiomics-based model for prediction of a composite endpoint, mainly LRC, can be improved by combination of primary tumor and lymph node radiomics.

Do we need standardized imaging protocols or robust radiomic features for the development of image-biomarker based prognostic models?

D. Vuong (1), M. Bogowicz (1), J. Unkelbach (1), R. Foerster (1), S. Denzler (1), A. Xyrafas (2), M. Pless (2), S. Thierstein (2), S. Peters (3), M. Guckenberger (1), S. Tanadini-Lang (1) for the Swiss Group for Clinical Cancer Research (SAKK)

(1) Department of Radiation Oncology, University Hospital Zurich, University of Zurich, Switzerland
(2) Swiss Group for Clinical Cancer Research (SAKK) Coordinating Center, Bern, Switzerland
(3) Department of Oncology, Centre Hospitalier Universitaire Vaudois (CHUV), Lausanne, Switzerland

Introduction

Radiomics is a promising tool for identification of new prognostic biomarkers. Radiomic models are often based on single-institution data. However, multi-centric data that are highly heterogeneous due to different scanning protocols reflect better the clinical reality. Robustness studies are crucial to find features independent from e.g. scanner settings. We studied if a CT radiomics overall survival (OS) model trained on multi-centric data with prior robust feature selection can achieve a similar performance as a model on standardized data.

Materials and Methods

Pre-treatment CT data from 121 stage IIIA/N2 NSCLC patients from a prospective Swiss multi-centric trial (SAKK 16/00, neoadj. chemo- or radiochemotherapy prior to surgery) were used to calculate 1404 radiomic features on the primary tumor. Two OS radiomic models were trained on (1) a standardized imaging protocol (native CT, standard kernel, n=84) and on (2) the entire heterogeneous dataset but with pre-selection of robust radiomic features. Robust features were extracted from four distinct robustness studies (contrast, convolution kernel, motion, delineation). Stability measure was the intra-class correlation coefficient (>0.9 considered stable). Principal component (PC) analysis was performed for feature selection and PCs describing in total 95% of data variance were selected. Features were selected separately for the entire and standardized dataset. The feature with highest correlation to the PCs served as a surrogate for the multivariate Cox model. Finally, backward selection was performed. Model performance was quantified using Concordance Index (CI). 10-fold cross-validation and bootstrap with resampling were used both to verify and compare model performances.

Results

Robustness studies revealed 113 stable features (n_{shape}=8, $n_{intensity}$=0, $n_{texture}$=7, $n_{wavelet}$=98). Strongest robustness influence was the convolution kernel. The final OS model on the entire non-standardized dataset consisted of four and the model on standardized data of six features (all identified as unstable). The model on standardized imaging data showed significant better prognostic performance compared to the model with robust feature pre-selection based on the entire heterogeneous imaging data (CI=0.64 and 0.61, $p<0.05$, resp.).

Conclusion

For our prognostic NSCLC radiomic models, image protocol standardization appears superior to using larger but heterogeneous imaging data combined with robust feature selection.

Modeling the radiation transport in a prototype MRI-Linac system using the Monte Carlo technique

Lukas Halter[1], Brendan Whelan[2], Brad Oborn[3], Natalia Roberts[3], Reto Kueng[4], Peter Manser[4], Michael K Fix[4], Marco Stampanoni[5], Paul Keall[2]

(1) Mobile Health Systems Laboratory, ETH Zurich, Switzerland
(2) ACRF Image X Institute, University of Sydney, Australia
(3) Centre of Medical Radiation Physics, University of Wollongong, Australia
(4) Division of Medical Radiation Physics and Department of Radiation Oncology, Inselspital, Bern University Hospital and University of Bern, Switzerland
(5) Institute for Biomedical Engineering, ETH Zürich and PSI, Villigen, Switzerland

Introduction

The Australian MRI-Linac project aims to develop real-time image-guided adaptive radiotherapy in order to improve the accuracy and thereby the outcome of radiotherapy. In this work, the development of a Monte Carlo (MC) model of the prototype MRI-Linac system is presented.

Materials and Methods

A model of the radiation transport was built by implementing the beam defining components of the MRI-Linac prototype into the Geant4 MC toolkit. The energy and the intensity distribution of the initial electron beam impinging on the target as well as parameters of the beam defining system were used to tune the MC model in order to match measured dose distributions.
First, a sensitivity study was performed determining the impact of different input parameter settings on the dose distribution. Second, measurements were performed with Gafchromic EBT3 films in a PMMA phantom and micro diamond in a homogeneous solid water phantom, respectively. Measured and calculated dose distributions were evaluated in terms of dose differences and gamma index evaluation.

Results

In the sensitivity analysis, it was found that the mean energy and the phantom placement significantly affect the shape of the PDD, while the shape of the dose profiles underwent characteristic changes for multiple parameters. Best agreement was achieved with an initial mono-energetic electron beam of 6.2 MeV, a spot size of 1.18 mm (FWHM) and a primary collimator opening of 5.7 mm. Using these parameters 91.25% of all dose values and 100% of the PDD passed a global gamma criterion of 2%/2 mm and 1%/1 mm, respectively.

Conclusion

The dosimetric results achieved in this work suggest a successful commissioning of an MC model for the prototype MR-Linac for which validation still has to be performed.

Anthropomorphic phantom with lung and liver compartments for MR guided radiation therapy

Emma Colvill, Miriam Krieger, Ye Zhang , Sairos Safai, Damien Weber, Tony Lomax, Giovanni Fattori

(1) Center for Proton Therapy, Paul Scherrer Institute, 5332 Villigen.

Introduction

Magnetic resonance imaging is widely recognised as a key element in many new frontiers of radiotherapy such as daily treatment adaptation and motion compensated dose delivery. Currently available phantoms for treatment quality assurance are however limited in realism and provide poor MR imaging texture. Therefore, renewed effort went to develop a solution for validating 4D CT and MR imaging and simulation of thoracic radiotherapy treatments.

Materials and Methods

We expand on an existing anthropomorphic breathing thorax phantom, by mimicking lung tissue using branching structures made up of blood vessels and airways making use of 3D printed flexible materials. Three elastic plastic planar inserts representing the bronchial tree and vasculature were covered in a polyorganosiloxane-based gel and sealed in ultra-thin plastic casing. The phantom is completed with a liver mould shaped by a thin casing of silicon, filled with gel and elastic plastic internal structures. Once fitted into a pre-existent ventilated lung phantom, stationary and 4D CT and T1 weighted MR imaging sequences were acquired to evaluate the structure visibility and mechanical properties of the thoracic phantom.

Results

Contrast of the 3D printed flexible plastic and the polyorganosiloxane gel was good on the T1 weighted MRI with image intensities of -500 - -400 and 0-100 respectively. The silicon liver casing had an image intensity range of 600 - 800. Good contrast is also confirmed on CT images with 0-150 HU for the printed plastic, 50 - 200 HU for gel and 650-800 HU for the silicon-based liver casing. The range of motion of the target was set to a relatively small 5mm during 4D imaging and the motion seen of the lung inserts ranged from 1-3 mm in the SI direction and 1-2 mm in the AP direction depending on the location in the lung. Similar ranges of deformation motion were seen for the liver phantom with larger motion at the tip and slightly smaller at the dome.

Conclusion

A ventilated thoracic dosimetry phantom has been updated to allow for enhanced imaging with MR and CT by the addition of lung inserts and a liver model. The addition of features within the lung and of a deformable liver will allow the reliable validation of 4D imaging techniques and treatments as well as deformable image registration quality assurance.

Deliverability-verification of treatment plans for dynamic mixed beam radiotherapy (DYMBER)

S. Mueller (1), P. Manser (1), W. Volken (1), D. Frei (1), A. Joosten (1), R. Kueng (1), E. Herrmann (1), O. Elicin (1), D.M. Aebersold (1), M.F.M. Stampanoni (2), M.K. Fix (1)

(1) Division of Medical Radiation Physics and Department of Radiation Oncology, Inselspital, Bern University Hospital and University of Bern, Switzerland
(2) Institute for Biomedical Engineering, ETH Zürich and PSI, Villigen, Switzerland

Introduction
Dynamic mixed beam radiotherapy (DYMBER) is a dosimetrically promising treatment technique utilizing increased degrees of freedom of a c-arm treatment unit. This includes different particle types (photons and electrons), dynamic gantry, table and collimator rotation and intensity and energy modulation. This work aims to verify the deliverability of DYMBER plans in terms of dosimetric accuracy, delivery time and collision avoidance.

Materials and Methods
An in-house developed treatment planning process is used to create DYMBER plans for a clinical brain and two head and neck cases consisting of photon dynamic trajectories and step and shoot electron apertures collimated without electron applicator but with the photon multileaf collimator (pMLC) at a reduced source-to-surface distance of 70-82.5 cm. Each DYMBER plan is delivered on a Varian TrueBeam to Gafchromic EBT3 films placed within an anthropomorphic head phantom. Dose distributions are calculated for the phantom using Monte Carlo simulations and compared to absolute film measurements by 2D gamma analysis using 2% dose difference relative to the maximal calculated dose and 2 mm distance to agreement criteria and a 10% dose threshold. Delivery time of each plan is determined starting from the first monitor unit (MU) until the last MU.

Results
All three DYMBER plans are successfully delivered to the films within the phantom without collision. The delivery times are 6.1, 6.3 and 7.0 min and the gamma passing rates are 99.9%, 99.2% and 99.6% for the brain and the first and second head and neck cases, respectively.

Conclusion
The DYMBER plans have successfully been validated on a phantom demonstrating the deliverability of DYMBER and the accuracy of c-arm treatment units and Monte Carlo dose calculations. This work was supported by Varian Medical Systems.

Abstracts – Oral presentations

Session Radiotherapy III

Towards personalized radiotherapy imaging dose report: a phantom-based evaluation of dose exposure

S. Thengumpallil (1) and K.H. Spruijt (1).

(1) Clinique des Grangettes, Radio-Oncology Department

Introduction

According to the revised ordinance on the radioprotection (ORaP) of this year, one of the points to fulfill for the radiation oncology department is the creation of a “radiation certificate”. This “radiation certificate” has to contain the estimation of the doses accumulated in the organs at risk (during treatment) and the dose to the patient accumulated during the imaging process. Besides imaging dose of the CT there is also Image Guided Radiotherapy (IGRT) dose. However, the latter is normally not available on treatment-planning system (TPS) and neither sent to the PACS. Within this context, we decided to find out a solution on this topic.

Materials and Methods

To evaluate the patient dose exposure, a CTDI body phantom with inserts for a CT ion chamber was used. Measurements were performed on a VARIAN Clinac iXS with On Board Imaging (OBI) system. Computed-tomography dose index (CTDI) and surface dose exposure were measured in Air Kerma for different values of tube voltage with a fixed current and exposure time for the different imaging modalities. The weighted CTDI was used as dose metric for CBCT, both full fan half arc and half fan full arc, while surface dose exposure for planar kV images and dose to water for MV images, the latter was calculated in Eclipse TPS by a 40x40 cm^2 field size at D max, for energies 6X, 18 X and 6FFF.

Results

From our measurements we calculated the weighted CTDI, surface dose exposure and dose to water for the different imaging modalities. Having those measurements, we created a fit of the dose metrics measured for kV, CBCT and a lookup table for the MV images and applied this to a created report in ARIA v13.7. This report contains all the imaging parameters (photon energy and mAs or #MU) applied according to the specific imaging modality.

Conclusion

We have created an automated report in ARIA which gives automatically an estimation of the dose coming from IGRT for each patient, for each treatment session and for each imaging modality. This report can be included in the patient’s file as record of the IGRT dose received during treatments. For the future, it would be interesting to make statistics of the recorded dose values from imaging per treatment type to improve the quality of the treatment, i.e. lowering the IGRT dose when possible.

Electromagnetic transponders for real-time tracking in lung stereotactic radiotherapy: first clinical experience

JACCARD M. (1), CAPARROTTI F. (1), DUBOULOZ A. (1), CHAMPION A. (1), RAKOTOMIARAMANANA B. (1), PICARDI, C. (1), PLOJOUX J. (2), SOCCAL P.M. (2), MIRALBELL R. (1) and DIPASQUALE G. (1).

(1) Department of Radiation Oncology, Geneva University Hospital, Geneva, Switzerland
(2) Department of Pneumology, Geneva University Hospital, Geneva, Switzerland

Introduction
We describe the clinical implementation of lung stereotactic radiotherapy (SBRT) using implanted electromagnetic transponders (EMT) for real-time tracking.

Materials and Methods
Four patients (pt) with early stage non-small cell lung cancer in the left lung were implanted with 2-3 EMT (Calypso™) in bronchi adjacent to the tumour. Simulation 4DCTs and free breathing (FB) CTs were acquired for all pts. A CT in deep inspiration breath hold (DIB) was also performed for one pt. We required 98% of the PTV (PTV_{FB}=ITV+5mm or PTV_{DIBH}= GTV+5mm, where ITV was defined from the GTVs from 4DCT) to be covered by 95% of the prescribed dose (60 Gy in 5 or 8 fractions). Treatment was delivered with two full or half volumetric modulated arcs and a 6 MV FFF beam. One pt was treaded in DIBH. Patients' setup in DIBH (resp. FB) at linac was performed using EMT position (resp. mean position) and CBCT verification. We analysed patient alignment and fractions delivery using DIBH or FB and real-time tracking with EMT.

Results
SBRT was successfully delivered using EMT. Visual inspection of CBCT before, during or after SBRT revealed good alignment of all structures and EMT. The median setup time was 10 min and 34 min at max, when Calypso™ captured small changes in target position due to pt reaction to table repositioning shift, requiring 4 CBCT to realign the pt and the target. The positions of EMT remained stable during DIBH treatments with median absolute shifts of 0.16 [0-0.43] cm. EMT positions were monitored real-time and automatic beam interruptions, triggered by detection of EMT positions out of tolerance (due to patient coughing or releasing of DIBH), occurred with a median [range] of 3 times per fraction [0-22]. The DIBH planning showed a clear dosimetric benefit compared to the FB technique.

Conclusion
Using Calypso for real-time tracking in lung SBRT allowed a fast and reproducible patient positioning and target monitoring. It permitted to treat small moving target with confidence, maximally sparing healthy lung tissue according to patient's breathing capability.

How risky is 4D planning? – A FMEA based human error comparison of planning risks in 3D/4D proton therapy QA performed at CPT/PSI

F. Emert[1], D. Pandya[2], J. Hrbacek[1], P. Morach[1], J. Rottmann[1], S. Zepter[1], L. Podofillini[2], A. Lomax[1], D.C. Weber[1], V.N. Dang[2]

[1]Center for Proton Therapy, Paul Scherrer Institute, Villigen, Switzerland

[2]Risk and Human Reliability, LEA, Paul Scherrer Institute, Villigen, Switzerland

Introduction

Identification and quantification of human error risks to minimize errors is of critical importance for patient safety in radiotherapy. As such prospective methodology for assessing risk in radiotherapy due to human interaction (Human Reliability Analysis, HRA) has been developed at our institute. As a case study, this has been used to compare failure risks of tasks in our newly developed 4D planning workflow to the more established 3D planning process.

Materials and Methods

5 tasks (3 specific for each workflow type, 2 common to both), their failure modes and causes (FC) were identified based on a HRA method developed at PSI, and screening analysis performed by 5 experts who are familiar with 3D/4D planning techniques. The risk estimation was based on the Failure Mode and Effect Analysis (FMEA) approach outlined in AAPM-TG100 report.

Results

Risk Priority Number (RPN) analysis of the tasks revealed a significantly higher risk of 4D compared to 3D planning processes. RPN ratios [RPN(4D)/RPN(3D)] for the two common tasks ranged from 1.2-1.9, whereas for the 3 workflow specific tasks, RPN ranged between 1.3-8.8. The top FCs that led to the highest risks were “less experienced with process” and “high workload”. High occurrence and low detectability were related to high RPNs.

Conclusion

Due to complicated 4D planning workflow and its relatively newness, significantly higher risks are observed in 4D tasks than their 3D counterparts. By studying complete failure scenarios using the inhouse developed HRA method we will investigate tasks with highest risks and minimize failure rates by the optimized distribution of QM/QA resources. The developed HRA method is also general and is applicable in conventional radiotherapy.

A quantitative evaluation of (deformable) image registration accuracy following AAPM TG 132

Philippe Logaritsch

Luzerner Kantonsspital

Introduction

To address the importance of questions regarding the validation, clinical integration and quality control aspects of image registration software the American Association of Physicists in Medicine (AAPM) has recently published their report No. 132 (*Use of image registration and fusion algorithms and techniques in radiotherapy).* In this work, which was carried out as part of the MAS in medical physics, practical aspects concerning the tests recommended in this report were investigated for the image registration software included in the treatment planning system used locally.

Materials and Methods

In addition to the report, the AAPM task group provided a number of digital phantoms that can be used to quantify the accuracy of image registration software. Due to the limited amount of data provided specifically for *deformable* image registration, in addition to the proposed test, further data was used. Namely, we employed 20 additional clinical CT datasets which are freely available (www.dir-lab.com) and which are used to benchmark various algorithms. Each of these datasets consists of a pair of lung CTs (inhale and exhale) and comes along with 300 preselected landmarks which can be used to evaluate the so called target registration error (TRE).

Results

The tests for rigid registration largely result in deviations within the recommended tolerances. The more interesting TRE-evaluation of the clinical datasets exhibits average errors between 1.05(±0.49) mm and 2.86(±4.71) mm while the maximal errors vary between 2.81mm and 28.33mm.

Conclusion

It can be concluded that the evaluated algorithm produces reasonably accurate results for the examined clinical datasets, comparable to results by similar studies. However, the rather strict tolerances of the TG 132 report are not always met.

ELPHA: Dynamically deformable liver phantom

Stefanie Ehrbar(1), Alexander Jöhl(1,2), Michael Kühni(2), Mirko Meboldt(2), Ece Ozkan Elsen(3), Christine Tanner(3), Orcun Goksel(3), Stephan Klöck(1), Jan Unkelbach(1), Matthias Guckenberger(1), Stephanie Tanadini-Lang(1)

(1) Department of Radiation Oncology, University Hospital Zurich and University of Zurich
(2) Product Development Group Zurich, Dep. of Mechanical and Process Engineering, ETH Zurich
(3) Computer-assisted Applications in Medicine, Dep. of Information Technology and Electrical Engineering, ETH Zurich

Introduction

Real-time adaptive radiotherapy of intrahepatic tumors needs to account for intra-fractional changes of the target location within the host organ due to motion and deformations of the liver. Phantoms representative of anatomical deformations are required to investigate and improve dynamic treatments.

Materials and Methods

An artificial liver with vascular structures was casted from soft silicone mixtures with radiographic and ultrasonic contrast. An actuator was used for compressing the liver in inferior direction according to a prescribed respiratory motion trace. Electromagnetic (EM) transponders integrated in our dynamically dEformable Liver PHAntom (ELPHA) help provide ground truth motion traces, which were used to quantify the motion reproducibility of the phantom and to validate motion tracking based on ultrasound imaging. To quantify the accuracy of ultrasound motion tracking, the dynamic vessel position in temporal sequences was compared to the EM transponder position by calculating the root-mean square error (RMSE). ELPHA was also used to investigate the dose deposition of dynamic treatment deliveries with plastic scintillation dosimeters (PSDs). PSDs allow for time-resolved measurement of the delivered dose, which were compared to the dose of the treatment planning system, both without and with motion compensation via treatment-couch tracking.

Results

Motion produced in ELPHA showed a high reproducibility with a submillimeter RMSE. The motion of the vasculature detected with ultrasound agreed with the EM transponder position with a RMSE below 1 mm. The agreement of the planned and measured PSD dose decreased with increasing motion amplitude. Without motion compensation, the dosimetric RMSE for a motion amplitude of 8, 16 and 24 mm was 1.2, 2.1 and 2.7 cGy/s, respectively. With couch tracking, these values decreased to 1.1, 1.4 and 1.4 cGy/s. This is closer to the static situation, with a RMSE of 0.7 cGy/s.

Conclusion

The developed liver phantom ELPHA features multi-modality image contrast, realistic breathing-induced motion and deformation, and includes a time-resolved dosimetry system. ELPHA was therefore suitable for quality assurance of real-time adaptive radiotherapy.

Implementation of an efficient in-house tool for patient-specific quality assurance in HDR brachytherapy

R. Kueng (1), D. Terribilini (1), V. Vitzthum (1), B. Isaak (1), M.K. Fix (1), M.F.M. Stampanoni (2), P. Manser (1)

(1) Division of Medical Radiation Physics and Department of Radiation Oncology, Inselspital, Bern University Hospital and University of Bern, Switzerland
(2) Institute for Biomedical Engineering, ETH Zürich and PSI, Villigen, Switzerland

Introduction
High dose rate (HDR) brachytherapy allows high conformity radiation therapy for a wide range of clinical indications, including breast cancer, cervical cancer or intra-operative radiotherapy. In our institution, a thorough pre-treatment quality assurance (QA) including independent dose calculation is part of the clinical brachytherapy workflow. With time for treatment planning and QA being a critical issue in HDR brachytherapy, it is of high importance to have a reliable and efficient pre-treatment QA tool at hand to conduct all the necessary checks. The purpose of this work is to implement an in-house tool for comprehensive QA for HDR brachytherapy applications.

Materials and Methods
Based on clinical demands, a QA software tool is implemented in the Python programming language with a Qt graphical user interface. The tool is designed for efficient QA workflow, including file import, plan verification, independent dose calculation and dwell position reconstruction verification, database access and PDF report generation. The tool is tested and evaluated for three clinical cases.

Results
The implemented tool proves to be feasible in clinical practice. The in-house solution provides the flexibility to implement all clinically requested features in a single, comprehensive tool. All features for a complete brachytherapy QA procedure are realized in the presented software application. Independent dose calculation agrees well with primary calculation of the planning system for the three test cases and independent dwell position reconstruction shows to be a valuable sanity check in pre-treatment QA.

Conclusion
A QA tool for HDR brachytherapy was successfully implemented in the Python programming language with a Qt based graphical user interface. The QA tool is currently being integrated in clinical environment.

Impact of tumor motion on robustness of radiomic features - comparison of PET and CT

F. Amstutz (1), D. Vuong (1), M. Bogowicz (1), M. Huellner (2), J. Unkelbach (1), P. Veit-Haibach (2), J. Kraft (1), M. Guckenberger (1), S .Tanadini-Lang (1)

(1) Department of Radiation Oncology, University Hospital Zurich, University of Zurich, Switzerland
(2) Department of Nuclear Medicine, University Hospital Zurich, University of Zurich, Switzerland

Introduction

Radiomics refers to the extraction of quantitative image features to describe tumor heterogeneity non-invasively, which can be used for predictive modelling. Respiratory motion can affect the absolute values of these features, makes them unstable and unsuitable for predictive modelling. The aim of this study was to compare the robustness of radiomic features derived from PET and CT images in terms of motion.

Materials and Methods

Two patient cohorts (CT and PET cohort, each n=10) with lung lesions were retrospectively selected. All patients had a pre-treatment 3D (average) and a 4D gated CT or PET on the same day. The exhale phase of the 4D acquisition was selected and compared with the average acquisition. The PET region of interests (ROIs) were segmented using semi-automated max SUV threshold-based method and the CT ROIs were manually delineated. In total, 1378 radiomic features were calculated with Z-rad radiomics implementation, i.e. shape (18), intensity (17), texture (137) and wavelet (1206). As a measure of the feature stability the intra-class correlation coefficient (ICC) was calculated between the average image and the exhale phase image for both modalities (ICC > 0.9 considered stable).

Results

The ROI center of mass motion was relatively small with a range of 0.81 mm (0.68 mm) to 4.48 mm (7.01 mm) for PET (resp. CT). Overall, only 24% and 27% of the features were stable for PET and CT, respectively. Intensity (65% vs 18%) and texture (50% vs 40%) features were more stable for PET than for CT. For both imaging modalities most stable were shape features (89%).

Conclusion

Motion affects both PET and CT based radiomics. The overall stability rate is similar, however for certain feature types (intensity and texture) PET radiomics was more robust than CT. It can be caused by steeper tumor-lung tissue gradient in CT in comparison to PET and thus larger averaging effects.

Abstracts – Posters

Contraindication for radiative deep regional hyperthermia for patients with large carbon implants

Marder D. (1), Poel R. (2), Gisep A. (3), Van Stam G. (1), Timm O. (1), Puric E. (1), Datta N.R. (1), Lutters G. (1)

(1) Kantonsspital Aarau, Radio-Onkologie-Zentrum KSA-KSB, Aarau, Switzerland
(2) Paul Scherrer Institute, Villigen, Switzerland
(3) icotec AG, Altstätten, Switzerland

Introduction
Hyperthermia to temperatures of 41-43°C has shown to be a valuable sensitizer for radiation- and chemo-therapy in cancer treatment. In this study the influence on specific absorption rate (SAR) and temperature by carbon fiber reinforced polyether-ether-ketone (CFR-PEEK) implants was investigated.

Materials and Methods
The influence on SAR and temperature was investigated in three rods with identical diameter of 5.5mm and length of 140mm. The rods were made of a titanium (TI), CFR-PEEK and PEEK of which the TI and the CFR-PEEK are commercially available products for trauma and reconstructive surgery provided by icotec AG, Altstätten, Switzerland. For the SAR measurements the samples were placed in a phantom inserted in the SigmaEye applicator of the BSD-2000 3D deep hyperthermia equipment (Pyrexar Medical, Salt Lake City, USA). Inside the phantom, a SAR probe (EASY4/MRI, SPEAG, Zürich, Switzerland) was moved along the samples and the relative SAR strength was recorded. For the temperature measurements, the samples were placed in a tissue equivalent gel. The temperature rise following a power pulse of 1000 W for 5 minutes (pulse#1) was measured.

Results
The SAR measurements parallel to the axis of the rods showed a clear increase of maximum relative SAR strength for both TI and CFR-PEEK but no increase for the PEEK material. Relative SAR increased by 329% for TI and 297% for CFR-PEEK at the tips of the rod. Temperature measurements in the gel phantom showed a similar behavior with a maximum temperature rise at the tips of the rod up to 27°C for both TI and CFR-PEEK and 3°C for PEEK after pulse#1.

Conclusion
TI and CFR-PEEK show a similar influence on SAR and temperature in a deep hyperthermia treatment set-up. Thus CFR-PEEK implants, like metal implants, must be a contraindication for radiative deep hyperthermia treatment.

VMAT applied to synchronous bilateral breast cancer radiotherapy: dosimetric study on DIBH versus FB set up.

D. Gaudino[1], S. Cima[2], M. Frapolli[2], D. Daniele[2], B. Muoio[2], G.A. Pesce[2], F. Martucci[2], N.C. Azinwi[2], D. Bosetti[2], L. Bellesi[1], M. Casiraghi[1], M.A. Piliero[1], F. Pupillo[1], A. Richetti[2], M.C. Valli[2], S. Presilla[1].

(1) Ente Ospedaliero Cantonale, Medical Physics Unit, Bellinzona, Switzerland.
(2) Oncology Institute of Southern Switzerland, Radiation Oncology, Bellinzona-Lugano, Switzerland.

Introduction
Bilateral breast cancer is a rare entity even if its incidence is increasing, due to the screening programs, and is about 2-5% of all breast malignancies. The definition of synchronous bilateral tumours (SBBC) coincides with diagnosis of both cancers within 6 months. Up to date no clear treatment guidelines for SBBC still exist even if small series or case report experiences have been published.
VMAT suits high dose homogeneity in such big volume and reduced treatment time compared to 3D-CRT and IMRT technique. Deep inspiration breath hold, when feasible, decreases lungs and cardiac acute and late toxicities. The aim of this study is to evaluate dosimetric parameters in SBBC patients treated with adjuvant RT by VMAT in order compare the DIBH and FB set up.

Materials and Methods
Computed tomography series of 14 patients were included in the study. All patients have been treated at the Oncology Institute of Southern Switzerland from 2011 to 2017 with conservative surgery plus sentinel node biopsy/axillary dissection and post-operative RT for invasive SBBC. For each patient two CT series, one in FB and the other one in DIBH modality were carried out. We evaluated two different planning approaches with and without breath hold modalities. The Mann–Whitney non-parametric test was used to compare the subgroups. Statistical significance was considered at $p<0.05$.

Results
The mean DVHs showed that the low, medium as well as the high dose region in the heart, the LAD and both lungs were reduced with DIBH. The average $Dmeanheart$ was reduced from 8.0 Gy (range 6-9.2) to 6.5 Gy (range 1.8-9.5) with the DIBH technique ($p=0.02$). The V25 showed a very low value in both techniques while $DMaxheart$ was reduced from 25.9 Gy (range 22.3-34.7) to 19.2 Gy (range 15.0-25.7) if DIBH ($p=0.006$). The $Dmeanheart$ was 6.49 Gy (range 4.8-9.5) if DIBH and 7.96 Gy (range 4.8-12.2) if FB ($p=0.02$). The value of FBDMaxLAD was 18 Gy (range 10.25-23.89) while the DIBHDMaxLAD was 14.5 Gy (range 9.29-19.21) with a significant difference ($p=0.02$).

Conclusion
The use of DIBH and VMAT technique improves heart, LAD and both lungs sparing in synchronous bilateral breast cancer adjuvant RT. We have been able to treat all patients with DIBH modality due to its feasibility and reproducibility. The OAR sparing is comparable with previous experiences and we have been able to respect the dose constraints considered for single breast RT. The clinical impact of this innovative technique on acute/late toxicities is under investigation.

Treating breast cancer with VMAT in deep inspiration breath hold: the Geneva experience

A. Dubouloz (1), P. Nouet (1), N. Koutsouvelis (1), G. Dipasquale (1), M. Jaccard (1), O. Fargier-Bochaton (1), M. Rouzaud (1)

(1) Radiation Oncology/Geneva University Hospitals, Geneva/Switzerland

Introduction
We report on the treatment management and the dosimetric results of deep inspiration breath hold (DIBH) volumetric modulated arc therapy (VMAT) treatments for breast cancer patients.

Materials and Methods
A total of sixty-four patients with breast cancer beneficiated from DIBH VMAT treatments since October 2016. The simulation CT (CTsim) room is equipped with the Real-time Position Management™ (RPM 1.7) Respiratory Gating (Varian) and the treatments are delivered on either a TrueBeam with Respiratory Gating or a Varian Linac with RPM. CTsim is acquired when the patient is able to maintain a reproducible and stable DIBH for at least 20 seconds. For dosimetric analyzis, patients were divided into 9 groups depending on the anatomical regions (breast and lymph nodes) included in the planning target volume (PTV), the breast laterality (50 left, 10 right and 4 double-sided irradiations) and the presence of a simultaneous integrated boost (SIB).

Results
In all groups, more than 95% of the PTV received at least 95% of the prescribed dose. The dose received by 2% of the PTV did not exceed 107.3% for groups without SIB, and 111.4% for groups with SIB. Mean dose (D_{mean}) to the heart was 5 Gy for groups without internal mammary chain (IMC) irradiation, and reached 8 Gy for double-sided breast and whole left breast with SIB irradiations. D_{mean} of the contralateral breast did not exceed 2.8 Gy for groups without IMC, and 3.8 Gy for groups with IMC. As for the contralateral lung: D_{mean} was 3 Gy and 5 Gy, V_{5Gy} was 20% and 40%, for groups without and with IMC respectively. For the homolateral lung, D_{mean} was 13.9 Gy for IMC+SIB groups, V_{5Gy} was below 50% for breast alone groups and below 78.7% for IMC+SIB groups.

Conclusion
Radiotherapy treatment of breast cancer using DIBH and a VMAT technique is more and more used in our center because of the excellent achievable OAR dose sparing and the good reproducibility of patient positioning.

Statistical assessment of intrafractional interruptions during DIBH left-breast treatments.

Lia Vugts, Sofia Celi, Nicoletta Lomax, Kirsten Steinauer, Gerd Lutters

Radio-Onkologie Zentrum KSA-KSB

Introduction

In our center left breast treatments are performed in Deep Inspiration Breath Hold (DIBH) monitored via Real-time Positioning Management (RPM) (Varian Motion Management System TB2.5). During the DIBH treatment the beam is automatically stopped if the patient inhales or exhales beyond a pre-set threshold. Such intra-fractional treatment interruptions have an influence on the treatment time and quality. A statistical study was conducted to investigate the intra-fractional interruptions and establish whether they can be linked to individual breathing patterns and/or systematical aspects of the treatment technique.

Materials and Methods

The RPM system records individual breathing curves from initial “beam on” to completion of the treatment of the field, including any interruptions and irradiation times. For this study an in-house statistical analysis program was used to calculate the number, frequency and length of the interruptions and link these data to different treatment aspects: the time length of the treatment fraction, the period of the treatment course, the evolution and deviations of the breathing pattern.

Results

Statistically interruptions appear to be frequent: 27% of the treatment fractions are interrupted at least once. However, an analysis of the interruption duration showed 58% of the interruptions to be insignificant (mean 1.3 s) and traceable to the DIBH treatment workflow. Other interruptions increase the treatment time by 50% in average. In general, breathing patterns do not stabilize over time: interruptions are only slightly more frequent during the first third of the treatment course than the rest of the course. A strong correlation could be established between the frequency of the interruptions and the deviation of a patient’s breathing curve during irradiation.

Conclusion

Intra-fractional interruptions of DIBH treatments are linked to individual breathing patterns, though the treatment workflow and oral commands play a role. Interruptions create longer treatment times, not only disrupting routine, but also reducing accuracy, thus potentially also treatment quality. A visual guiding system could reduce the impact of these disrupting factors.

GLAaS absolute dose calibration algorithm with Elekta iViewGT Electronic Portal Imaging Device (EPID): multi-institute first experiences.

Eugenio Vanetti (1), Marco Esposito (2), Juan Maria Perez (3), Stefano Ren Kaiser (4), Giorgia Nicolini(1)

(1) Radiqa Developments, Medical Physics Team, Bellinzona, Switzerland
(2) SC Fisica Sanitaria, Usl Toscana centro, Firenze, Italy
(3) Servicio de Radiofísica, Hospital Universitario HM Puerta del Sur, Móstoles (Madrid), Spain
(4) Servizio di Fisica Sanitaria, Fondazione Poliambulanza Istituto Ospedaliero, Brescia, Italy

Introduction

Radiotherapy with intensity modulation implies the setup of adequate QA programs to guarantee safe treatments. Amorphous silicon EPID technologies are particularly interesting due to their high spatial resolution, large area, stability, dynamic range, and real-time acquisition capabilities. In this context, the GLAaS[1] algorithm has proved capable to meet a variety of applications with a simple direct calibration process to convert raw measurements into absorbed-dose-to-water; nevertheless, GLAaS was never validate with a different technology apart from Varian-EPIDs. To test its feasibility out of single manufacturer environment, GLAaS was applied to Elekta iViewGT images.

Materials and Methods

Dosimetric data for 6MV beams from 3 different institutes (two Synergy and a Versa HD Elekta linacs) were collected at dmax and SDD=160cm (EPID position), for primary and transmitted radiation to be correlated with iViewGT pixel reading (R) and configure GLAaS algorithm. For open and modulated fields, comparison to TPS dose maps (Monaco-MC, RayStation-CC) was assessed through profiles and gamma analysis (local and global criteria).

Results

For a given beam, the response of iViewGT was confirmed linear, as already established for Varian EPIDs. Similarly, pixel-by-pixel response changes in time differentiating on field and/or segment sizes and beam quality, i.e. primary or below MLC radiation, basis were modelled. The satisfactory GLAaS algorithm configuration allowed pre-treatment QA verifications in all the three centers; a variety of cases, IMRT and VMAT, were analysed.

Conclusion

The extension of GLAaS algorithm to iViewGT - EPID offers the opportunity to easily set-up flexible and reliable verification. Moreover, the high resolution of EPID is of interest in highly demanding conditions such as for SRS / SBRT treatments and/or complicate fluence pattern. Indeed, the GLAaS approach allows a straight comparison between EPID measurements and TPS water dose maps (calculated with the same algorithm used for patient).
The GLAaS compatibility with different technologies could offer a measurement tool in multi-institute studies concerning treatment delivery and dose calculation issues.

Suitability of DDC for CT protocol optimisation with abdominal and head phantom

Christian Sommer (1), Ismail Oezden (2), Thiago Lima (2), Mathias S. Weyland (1), Gerd Lutters (2), Stephan Scheidegger (1,2)

(1) ZHAW School of Engineering, Winterthur, Switzerland
(2) Kantonsspital Aarau, Switzerland

Introduction
Assessing image quality of CT scans regarding clinical use is challenging. We propose an approach using a difference detail curve (DDC) phantom for abdomen and head in combination with a radiation dose chamber.

Materials and Methods
Novel DDC phantoms have been developed. The phantom family is based on a cylindrical DDC insert containing low contrast objects with different area sizes, representing native or contrast media enhanced structures. This insert can be used in combination with abdominal- or head phantoms. The abdominal phantom consists of elliptical PMMA slices with different effective diameters. The head phantom consists of a 3D printed skull (bone-equivalent material), casted in epoxy. The phantoms were scanned with different Computed Tomography Dose Index ($CTDI_{Vol}$) levels, scan protocols (abdomen and head) and two different tube voltages. Dose modulation was disabled. The dose length product (DLP) was measured simultaneously with a 30 cm ionisation chamber. Up to four human observers performed the DDC evaluation of the acquired images. For the analysis, a dedicated Python-based software package was developed. Data of 1040 measurements from 16 different CT units have been analysed.

Results
The DDCs acquired consistently exhibit properties in line with theory, e.g. a dose dependency for low contrast detectability. We also found a linear relation between the minimal observed contrast for a given diameter and the $CTDI_{Vol}$. Furthermore, the curves corresponding to the abdominal phantoms of different size were coinciding, indicating that the same image quality was achieved, although with different doses. Lastly, the required contrast for a given contrast object detectability varies strongly between the different institutes and CT units.

Conclusion
The DDC is a suitable method to evaluate the influence of specific parameters (such as abdominal diameter) on image quality with respect to the dose. With the use of a larger dataset as a DDC reference catalogue, it will be possible to optimise protocols regarding image quality and dose.

Multi-dimensional analysis of OSMS data during DIBH treatments

H. Schneider, N. Lomax, G. Lutters

(1) Radio-Onkologie-Zentrum KSA-KSB

Introduction
Deep Inspiration Breath Hold (DIBH) is used to avoid high dose deposition in the heart during left breast radiotherapy treatment. Some studies show the dosimetric impact of DIBH treatment. However, the real movement during the patient treatment, taking the multidimensional movements into account, has rarely been studied directly. An Optical Surface Management System (OSMS), Varian, opens up the possibility of investigating the surface spatial movements before and during treatment.

Materials and Method
90 left breast cancer patients undergoing DIBH radiation therapy (Truebeam, Varian) were monitored by an OSMS. The resulting 1893 treatments were evaluated in terms of the improvement between normal breathing and the DIBH. Furthermore the ability and duration of breath-hold after reaching the deep inspiration level was recorded.

Results
The vertical movements between the normal breathing phase and the DIBH phase were 7.4 ± 2.1mm (long. 6.2 ± 3.9mm, lat. 4.3 ± 2.1mm). After one or two breathing training cycles without radiation the treatment phase started with a duration of 15 ± 3.5s and a vertical movement of 0.8 ± 0.7mm as well as longitudinal and lateral (0.8 ± 0.7mm, 0.57 ± 0.5mm) during this DIBH phase. The breath-hold ability and the vertical amplitude did not change significantly over the whole treatment duration.

Conclusion
The OSMS used in the clinical routine to treat DIBH patients enables the multidimensional monitoring of patient surface motions. Without using assisted breathing techniques, we have not been able to record such high vertical gain compared with the normal breathing cycle as reported in other publications. However, the estimated treatment position could be maintained within a small range by almost all patients and the OSMS helps to reduce the positional uncertainties during treatment.

Evaluation of the pre and post-treatment positioning accuracy of patients treated in Gantry 2

L.Mikroutsikos, L.Marc, F.Albertini, D.C. Weber, T.Lomax, A.Bolsi,

Paul Scherrer Institute

Introduction

In 2014, the newly in-house developed Gantry 2 (G2) treatment machine has started clinical operation. New couches and new immobilization components have been designed to treat patients in G2. As with proton therapy, applied dose gradients can be steep, accurate patient positioning is extremely important. This study performs a retrospective analysis of the positioning of all patients treated in G2, and compares it with the results obtained for the positioning of the patients treated in the older Gantry 1 (G1) treatment machine.

Materials and Methods

Patient positioning is based on two orthogonal topograms acquired with the CT-on rails scanner in G2 room: the measured differences between daily and reference images acquired together with the planning CT are used to define daily positioning corrections to the patient table in the treatment room. The patients (174) were stratified based on the immobilization devices and the localization of the tumor. Systematic (Σ_x, Σ_y and Σ_z) and random errors along each direction (σ_x, σ_y and σ_z) have been computed for each patient subgroup. Random errors were combined to compute $\sigma_{85\%}$, defined as the random error probability of 85% of the positioning error in the respective stratified group of patients. Additionally, to estimate possible patient movements during table movements and irradiation, post-treatments topograms are periodically acquired and compared with the pre-treatment topograms of the day. Those results computed for the patients treated in G2 were compared with the results for the G1 patients, which have been analyzed separately for the patients (301) treated in the period between 2009-2012 and 2012-2018 (490).

Results

The analysis of the results showed an improvement for G2 compared to G1 for both positioning ($\sigma_{85\%}$ of 2.00 mm for G2, 2.22 mm for G1) as well as post-treatment control data ($\sigma_{85\%}$ of 1.29 mm for G2, 1.82 mm for G1). The positioning proved to be more accurate in G2 for every immobilization device and localization of the tumor. Additionally G1 positioning was reproducible when comparing the results of 2012 and 2018.

Conclusion

An improvement in the patient positioning accuracy, as the one observed in G2, is one of the fundamental factors to guarantee high accuracy in proton therapy.

EPR-Imaging of magnetic field induced dose effects at air cavities

Sebastian Höfel (1,2), Michael K. Fix (3), Felix Zwicker (2), Malte Drescher (1)

(1) Department of Chemistry, University of Konstanz, Germany
(2) Klinik für Strahlentherapie/Radiologische Gemeinschaftspraxis, Gesundheitsverbund Landkreis Konstanz, Konstanz, Germany
(3) Division of Medical Radiation Physics and Department of Radiation Oncology, Inselspital, Bern University Hospital and University of Bern, Switzerland

Introduction

New hybrid radiotherapy treatment systems combining a MRI-scanner with a linear accelerator are currently introduced into clinical practice. The necessary strong magnetic fields of MRI may considerably affect radiation dose distributions, especially at air-interfaces due to the electron return effect (ERE). The goal of this work was to examine the feasibility of EPR Imaging (EPRI) to visualize magnetic field induced changes of dose distributions at air-cavities.

Materials and Methods

Air-filled fused quartz tubes (I.D. of 3-4 mm) were placed inside a PMMA phantom and irradiated by a 6 MV photon beam of a Tomotherapy® treatment system to doses of up to 600 Gy. The irradiations were performed in the absence or presence of a transverse, homogeneous magnetic field of around 1 Tesla. For this purpose, an in-house permanent magnet was used. The 2-D spatial distribution of radiation induced, stable defects in the quartz were subsequently detected by applying spin echo detected EPRI. A signal – dose calibration enabled us to convert the defect density to dose.

Results

The EPR signal amplitude showed a near linear increase with dose. After 22-24 hours of measurement the SNR was sufficient to reconstruct images with high spatial resolution (below 100 µm). We measured magnetic field induced changes of the dose distribution inside the quartz tubes ranging from -25% to + 25%.

Conclusion

Our results show the feasibility of spin-echo detected 2D-EPRI to depict magnetic field induced dose effects at small air cavities (diameter 3 - 4 mm). With regard to EPRI, fused quartz serves as a suitable probe material for measuring spatially highly resolved radiation dose distributions, yet high doses are needed to obtain a sufficient signal-to-noise ratio.

Portal Dosimetry with the 43 cm x 43 cm MV Imager: Improving Large-Field Performance by Diagonal Profile Adjustments

Thomas Buchsbaum (1), Federico Hasenbalg (1)

(1) Stadtspital Triemli Zürich, Radio-Onkologie, CH-8063 Zürich

Introduction

Varian's Portal Dosimetry is an important part of our patient-specific quality assurance procedures for intensity-modulated treatment plans on our TrueBeam 2.7 machines. The current 43 cm x 43 cm MV imager (DMI) improved significantly compared to its predecessor, the AS1000 imager, with respect to dose- and dose-rate dependence, and arm backscatter effects. With the standard calibration, however, we experienced a drop in the performance (gamma analysis passing rates) for flattened beam modes (6X, 10X, and 15X) when field sizes were large: the difference between predicted and measured dose increased with the distance to the imager center. FFF modes did not suffer from this effect.

Materials and Methods

We assumed a distance-proportionate scaling of the diagonal profiles used for the calibration of the portal dose image prediction (PDIP 15.1.51) models:
Scaling $s(r) = 1 + f(E) * r / (20\ \text{cm})$, where r is the radial distance and f the energy-mode dependent scaling parameter. We estimated f based on the measurements of a shifted version of Varian's PDIP calibration fluence and a large-field VMAT treatment plan.

Results

Our estimates for the scaling parameters f are 0.042 for 6X and 10X, and 0.064 for 15X; which corresponds to a 4.2% (6.4%) scaling at a diagonal profile distance r = 20 cm. Our clinical PDIP models are calibrated using these scaled diagonal profiles. We will present field-size dependent performance statistics (gamma analysis passing rates) of our patient-specific plan verifications.

Conclusion

The distance-dependent modification of the diagonal profiles used for PDIP calibration resulted in Portal Dosimetry models that give reliable results for small and large-field IMRT- and VMAT treatment plan verification.

Hybrid Intensity Modulated Treatment based on Gradient Fluence Maps: Application to loco regional breast cancer

R. Boucenna, ***N. Pitteloud****, M. Betz*

Clinique Bois-Cerf Hirslanden Lausanne

Introduction

Radiotherapy for breast cancer including nodal areas can lead to coverage difficulties and exposes organs at risk to higher radiation doses. In addition, modern modulated treatments may significantly increase volumes receiving low doses. The purpose of this planning case report is to share the dosimetric results of an innovative hybrid Intensity Modulated Therapy for loco regional breast cancer. The breast volume is treated by IMRT tangential fields, and the nodes are treated by VMAT. Both techniques are used conjointly and safely through the creation of Gradient Fluence Maps.

Materials and Methods

Two patients with a loco regional breast cancer were selected to evaluate the hybrid modulation technique for the left and right side. For each patient, two clinical situations were examined. The first situation included breast, supraclavicular, infraclavicular and axillary lymph nodes as target volumes. The internal mammary chain was added to the second one. The following metrics have been reported: the conformity index and the $V_{95\%}$ for targets volumes; V_{30}, V_{20}, V_{10}, V_5 and D_{mean} for the ipsilateral lung; D_{mean} and D_{max} for the contralateral organs at risk (lung and breast) and V_5 and D_{mean} for the heart.

Results

For all 4 clinical situations, $V_{95\,\%} \geq 90\%$ and a conformity index of approximately 1.2 were found for all target volumes. The contralateral organs at risk received mean doses in the range of [1, 2] Gy and D_{max} of approximately 10 Gy. For the ipsilateral lung, the V_{30} was in the range of [10, 15] %, V_{20} = [15, 20] %, V_{10} = [20, 30] %; V_5 = [35, 45] %, D_{mean} = [8, 10] Gy. For the heart, in the case of right breast treatment V_5 = [1, 8] % and D_{mean} = [1, 2.5] Gy. For the left, V_5 = [5, 10] % and D_{mean} = [2, 3] Gy.

Conclusion

The large volume receiving the low dose in the contralateral organ at risk can be limited with hybrid modulation, while insuring clinically acceptable nodal and breast target coverage. Dosimetric results for the heart and ipsilateral lung are comparable to other standard modulated techniques such as VMAT or IMRT.

Dosimetric Impact of Titanium and Carbon Implants in Photon Therapy

N. Klippel (1), D. Terribilini (1), A. Gisep (2), A. Joosten (1), H. Hemmatazad (1), K. Zaugg (3), D.M. Aebersold (1), P. Manser (1)

(1) Division of Medical Radiation Physics and Department of Radiation Oncology, Inselspital, Bern University Hospital, Switzerland
(2) icotec AG, Altstätten, Switzerland
(3) Klinik für Radio-Onkologie, Stadtspital Triemli, Zürich, Switzerland

Introduction
Metal implants create artefacts in planning CTs, which compromise image quality, and thus contouring and dose calculation in radiation therapy. In this study, the effects of carbon/PEEK composite implants on the radiation process with photons is investigated.

Materials and Methods
A unique upper body phantom with the following interchangeable inserts was used: (1) native spine, (2) titanium pedicle system, (3) carbon/PEEK pedicle system, (4) carbon/PEEK system with titanium tulips. After CT scans, PTVs were contoured for the following cases: (1) a palliative setting with the spinal cord included in the PTV, (2) a spine metastasis with paraspinal tumor extension irradiated with curative intent and sparing the spinal cord. Conformal plans and VMAT plans with a fraction dose of 2 Gy were created with the Varian Eclipse planning system. All plans used 6 MV photons and were delivered on a Varian Unique linac. We measured the dose distribution close to the implants with GafChromic films in a frontal plane of the phantom.

Results
In the case of a single dorsal static field, the disturbance by titanium implants results in hot and cold spots with dose deviations up to 20% of the dose that is expected without implants. The treatment planning system is not able to fully reproduce this behavior. The effect becomes smaller with increasing complexity of the applied treatment plans: In a conformal plan consisting of two dorsal fields, the measured dose deviation for the titanium implant is 10%. The applied VMAT plans were less influenced by implants. For pure carbon/PEEK implants, dose deviations in the measurement plane are lower than 5% for all plans. Carbon/PEEK implants lead to very similar dose distributions compared to calculations without implants.

Conclusion
Titanium implants cause measureable dose deviations, which depend on plan complexity. Implants with carbon/PEEK material can minimize these deviations.

Shortening delivery times for PBS proton therapy by reducing the number of proton spots without compromising dosimetric plan quality

Maria F. Belosi, MSc [1]; Steven van de Water, PhD [1], Francesca Albertini, PhD [1]; Damien C. Weber, MD [1]; and Antony J. Lomax, PhD [1]

[1] Center for Proton Therapy, Paul Scherrer Institute, 5232 Villigen PSI, Switzerland

Introduction

Spot-scanned (PBS) proton therapy could benefit considerably from shorter delivery times, especially when treating large volumes or moving targets (using re-painting or breath-hold techniques), or when applying hypo-fractionation. Delivery times for PBS proton therapy treatment plans can be shortened by reducing the number of proton spots while maintaining dosimetric plan quality. Because a strongly reduced number of spots can potentially affect the treatment delivery, we assessed the deliverability, delivery accuracy, robustness and actual delivery time reduction of a spot-reduced treatment plan.

Materials and Methods

For a head-and-neck cancer patient, conventional and 'spot-reduced' single-field uniform dose (SFUD) plans were generated, with the spot-reduced plan being optimized using the 'pencil beam resampling' technique. This involves repeated inverse optimization while iteratively excluding low-weighted proton spots until the plan quality deteriorates. Beam setup was identical for both plans and the resulting dosimetric plan quality was comparable. Both plans were delivered on the PBS Gantry 2 at PSI, measuring the delivery time per field and dose profiles in water. Subsequently the delivered 3-D dose distributions were reconstructed using machine log-file information. In addition, robustness analysis was performed to assess sensitivity to delivery inaccuracies and errors in patient setup and proton range.

Results

The total number of spots for the plan could be reduced by 95% (from 33855 to 1510) resulting in an average delivery time reduction of 44% per field (from 51.0 s to 28.7 s). For both plans, measured dose profiles in water differed from the planned dose by <2% and the log-file dose reconstruction was within ±1% of the planned dose for all voxels. As expected, the spot-reduced plan was slightly more sensitive to delivery inaccuracies, requiring a spot position accuracy within ≤0.5mm, but were surprisingly less sensitive to setup and range errors.

Conclusion

Delivery times per field could be reduced by 44% using spot reduction without substantially compromising plan quality, delivery accuracy or robustness.

Brain sparing through iterative single isocentre planning for multiple brain metastases

Nicoletta Lomax, Sara Alonso, Mauricio Leick, Susanne Rogers, Gerd Lutters

Radio-Onkologie-Zentrum KSA-KSB, Kantonsspital Aarau

Introduction

As linac-based radiosurgery (RS) for multiple brain metastases (BMs) becomes more widely used, single isocentre techniques are desirable for improved efficiency. In clinical practice however, the use of a single isocentre is often limited by geometrical distribution of the metastases, dose to critical organs and risk of radionecrosis (V10Gy (brain – GTV) < 10cc is our constraint for single fraction RS). The aim of this study was to compare the Elements Multi Metastases (BrainLab Ltd) automatic planning modules Versions 1.5 (MM1.5) and 2.0 (MM2) and to the evaluate the potential of MM2 to overcome these issues and increase the number of cases for which a single isocentre treatment is viable.

Materials and Methods

20 cases (each with 2-10 BMs, total of 85 BMs) were planned with MM1.5 using a single isocentre and dynamic conformal arcs with a dose of 20Gy to 99% of the PTV volume and were replanned with MM2. MM2 allows a degree of user intervention, so that for each case, 3 plans were optimised with the "normal tissue sparing" (NTS) parameter set to low, standard and high and critical organ sparing if required. Plan quality metrics (conformity index CI, gradient index GI, V10Gy (brain – GTV for each BM), mean dose, maximum dose relation MDR (often termed prescription isodose level)) were analysed.

Results

The linear relationship between V10Gy and PTV volume with different planning optimisation parameters is shown. V10Gy is consistently reduced when planned with MM2 compared with MM1.5. Increasing the NTS both increases the mean and maximum PTV doses and further reduces the V10Gy. For MM1.5 mean MDR = 83%, for MM2, mean MDR = 84%, 78%, 75% for NTS settings low, standard and high respectively. Case studies also demonstrated personalised GTV-PTV margin adaption and OAR sparing with MM2.

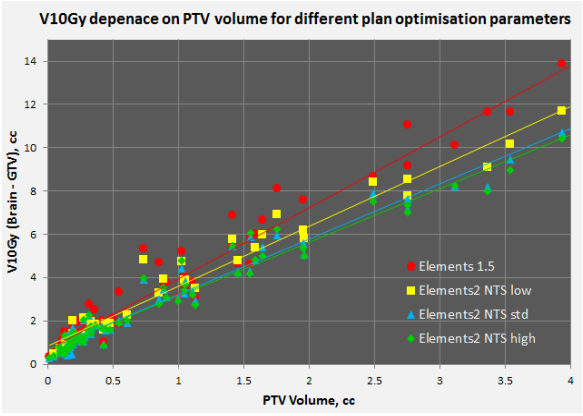

Conclusion

The lower V10Gy achievable using MM2 may allow a larger volume of BMs to be treated safely with a single fraction, where otherwise hypofractionation would be necessary.

Supine or prone-crawl photon and proton RT plans for breast and regional lymph node including the IM chain

Francesca Belosi[2, $], Bruno Speleers[1,$], Werner De Gersem[1], Pieter Deseyne[3], Leen Paelinck[3], Alessandra Bolsi[2], Anthony Lomax[2], Bert Boute[5], Annick Van Greveling[3], Christel Monten[1,3], Joris Van de Velde[4], Tom Vercautere [1,3] , Liv Veldeman [1,3], Damien Charles Weber[2,6] and Wilfried De Neve [1,3,$]

[$]contributed equally

[1]Department of Radiotherapy and Experimental Cancer Research, Faculty of Medicine and Health Sciences, Ghent University, Belgium

[2]Paul Scherrer Institut, Villigen, Switzerland

[3]Department of Radiation Oncology, University Hospital Ghent, Belgium

[4]Department of Anatomy, Faculty of Medicine and Health Sciences, Ghent University, Belgium

[5]Industrial Design Center, Faculty of Engineering and Architecture, Ghent University, Belgium

[6]Radiation Oncology, University Hospital of Bern, Inselspital, Bern

Introduction

A specifically adapted prone patient support device, resembling a phase of the crawl swimming stroke (prone-crawl position) to obtain unobstructed beam access to treat the whole breast (WB) and lymph-nodes (LNN), including the MI-chain (MI) has been developed at Ghent University Hospital (GUH, Belgium). This device offers the advantages of significantly reducing heart and lung doses as compared to the supine setup. The aim of this study was to compare effectiveness of prone-crawl position for treating WB and LN using photon and proton irradiation

Materials and Methods

Planning CTs were acquired at GUH for 6 left sided breast cancer patients both in supine and crawl position. Photon plans were created with supine coplanar or prone non-coplanar multiple overlying partial arc VMAT using integrated planning tools in the GRATIS treatment planning platform (Sherouse systems, Inc., Chapel Hill, USA). Proton plans were made at Paul Scherrer Institute (PSI) using pencil beam scanning IMPT. Three oblique fields from below the treatment couch (anterior to the patient's breast) were used for the prone, and one direct anterior with 2 oblique 'narrow angle' fields for the supine position. Each field was calculated on a union of the 3 individual targets (WB/LNN/MI). Finally the weights of the pencil beams (PBs) of all fields were optimized together so to achieve the most homogeneous dose distribution to the separate targets. Dose prescription was 2.67 Gy or Gy(RBE)/fx for 15 fractions.

Results

Target coverage was comparable among all techniques with a significantly higher minimum dose in proton plans, being 39.03 Gy(RBE) vs 37.07 Gy for the MI PTV, 38.20 Gy(RBE) vs 37.09 Gy for the LNN PTV and 38.34 Gy(RBE) vs 37.04 Gy for the WB PTV. Average mean heart dose for supine and prone-crawl plans was 5.6 [3.5-8.8] Gy and 4.3 [3.0-5.6] Gy, for photons ($p=0.16$) and 1.02 [0.6-1.6] Gy(RBE) and 1.08 [0.6-1.9] Gy(RBE) for protons, respectively ($p=0.8$). The average mean bilateral lung dose for supine and prone-crawl plans was 5.91 [4.1-7.8] Gy and 2.90 [2.1-3.9] Gy, for photons ($p=0.002$), and for protons 1.56 [1.1-2.0] Gy(RBE) and 1.09 [0.7-1.7] Gy(RBE), respectively ($p=0.016$). Differences between photons and protons were highly significant ($p<0.001$).

Conclusion

Prone-crawl position for the treatment of WB-LNN-MI allowed significantly lower lung dose exposure compared to the standard supine setup for photon plans and a lower mean heart dose. Proton plans were superior to photon plans and obtained a higher minimum dose to the PTV, and improved dose homogeneity for breast and nodal targets, as well as substantially lower mean heart and lung dose.